Uncued and cued dynamics measured by response classification

Steven S. Shimozaki

School of Psychology, University of Leicester, Leicester, United Kingdom

Attention as a serial contiguous spotlight has met challenges from parallel-noisy models and evidence that attention can split across multiple locations. To assess this question, this study compared the dynamics at cued and uncued locations during a cueing task through response classification. Four observers performed a yes/no contrast discrimination of Gabors appearing at two locations, with simultaneous cues appearing at one location with 80% validity. Stimuli were presented for 272 ms in 'contrast noise'; the peak contrasts of the Gabors varied randomly across 12 intervals of the stimulus duration. Response classification yielded a 'classification number' for each location (cued and uncued) and interval, giving two classification number functions (cued and uncued) across the stimulus duration. Serial models predict delays in the uncued functions, whereas parallel models do not. No evidence for delays at uncued locations was found, with no significant differences for the amplitude-matched cued and uncued functions, or for the functions' peak times after smoothing with third-degree polynomials. Also, the relative integrals between the cued and uncued functions were fit well to a parallel-noisy weighted likelihood model assuming a linear summation of responses across intervals. Thus, a parallel description of attention seemed to best explain the results in this study.

Keywords: computational modeling, temporal vision, search, visual attention, cueing, response classification

Citation: Shimozaki, S. S. (2010). Uncued and cued dynamics measured by response classification. *Journal of Vision, 10*(8):10, 1–27, http://www.journalofvision.org/content10/8/10, doi:10.1167/10.8.10.

Introduction

Two paradigms have had a significant impact on visual attention research, visual search and cueing. In a classical visual search task, an observer must detect or localize a signal in a field of distractors (nonsignal items that might be mistaken for the signal). The classic result is the 'set size' effect, in which performance decreases with increasing number of items (set size). The second paradigm is the cueing task, in which the observer must detect a signal appearing at two or more locations and receives a cue (usually before the stimulus) indicating the likely location of the signal. The classic result for the cueing task is the cue validity (or just cueing) effect in which valid cues have better performance and invalid cues have worse performance than nonpredictive or neutral cues. Across both these paradigms, a common and intuitive description of visual attention to explain set size and cueing effects is a single contiguous attentional area (or spotlight) that improves vision, at a cost to the vision at unattended areas, and that must be moved serially from location to location. For set size effects, the increasing set size demands more locations to be attended serially, and for cueing effects, attention is drawn to the cued location at a cost to the uncued location. The serial limited capacity 'spotlight' model of attention was ubiquitous in earlier visual attention research (Feature Integration Theory: Treisman & Gelade, 1980; Enhancement: Posner, 1980; Zoom Lens: Eriksen & Yeh, 1985; Eriksen & St. James, 1986) and still remains common in more recent research (e.g., Guided Search, Wolfe, 1994, 2007; Wolfe, Cave, & Franzel, 1989; Wolfe & Gancarz, 1996). Also, recent studies have measured accuracy as a function of response time, or speed-accuracy tradeoff curves, with a deadline procedure requiring speeded responses at different times (Carrasco, Giordano, & McElree, 2004, 2006; Carrasco & McElree, 2001). These studies suggest that cued (attended) locations have speeded processing compared to uncued (unattended) locations, consistent with a limited capacity hypothesis of attention.

However, recently a number of studies have suggested that attention may be split across multiple locations. Generally, these studies find cueing effects for non-contiguous cued areas without finding cueing effects for areas between the cued areas, either perceptually (Awh & Pashler, 2000; Bichot, Cave, & Pashler, 1999, Experiment 6) or through assessment of neural activity (fMRI: McMains & Somers, 2004, 2005; Visually Evoked Potentials, or VEP: Müller, Malinowski, Gruber, & Hillyard, 2003). These results clearly oppose the suggestion of a single contiguous attended area. Another study by Kramer and Hahn (1995) found that distractor letter stimuli appearing without a sudden onset could be ignored when appearing between non-contiguous cued locations. Also, signal detection theory and ideal observer models propose an alternative to limited capacity and/or serial accounts of visual attention (Eckstein, Shimozaki, & Abbey, 2002; Eckstein, Thomas, Palmer, & Shimozaki, 2000; Kinchla, 1974; Kinchla, Chen, & Evert, 1995; Palmer, 1995;

doi:10.1167/10.8.10 Received August 20, 2009; published July 20, 2010 ISSN 1534-7362

Palmer, Ames, & Lindsey, 1993; Palmer, Verghese, & Pavel, 2000; Shaw, 1980, 1982; Shimozaki, Eckstein, & Abbey, 2003; Verghese, 2001). These models are characterized generally by assuming no loss of visibility at unattended locations (i.e., equal signal-to-noise ratios at all locations), and by assuming responses to each stimulus that are subject to internal noise; thus, the models are often known as 'parallel-noisy' models of attention. The models predict set-size effects and cueing effects despite having no limited capacity or seriality in their attentional processing. Parallel-noisy models predict set size effects by the increased decisional noise summed across increasing items, and predict cueing effects through the use of larger weighting or scaling of the cued location (usually through a Bayesian calculation of prior probabilities). It should be noted that the parallel-noisy models cannot predict results from several attentional phenomena, including cueing effects from nonpredictive cues (such as those used in attentional capture studies, e. g., Folk, Remington, & Johnston, 1992, Experiment 3; Jonides, 1981, Experiment 2; Theeuwes, 1991) and differences between voluntary and involuntary attention (e.g., Jonides, 1981; Müller & Rabbitt, 1989; reviewed by Wright & Ward, 2008). However, there are several studies that demonstrate that the parallel-noisy models do predict set size (Palmer, 1995; Palmer et al., 1993) and cueing effects with predictive cues (Eckstein et al., 2002; Shimozaki et al., 2003) well in certain cases. At a minimum, the parallel-noisy models suggest caution in assuming that set size and cueing effects *directly* imply a limited-capacity serial attentional model.

This study aims to assess the temporal dynamics of attention through the response classification technique, and specifically the potential differences at the cued (attended) and uncued (unattended) locations in a cueing task. Response classification (classification images) is based upon how response outcomes are driven by noise added to the stimulus, and estimates the amount of information used in a task. Generally, a serial model predicts that information use at the uncued location will be delayed, compared to the cued location, while a parallel model does not predict such a delay. Response classification was developed by Ahumada and Lovell (1971), and is the behavioral equivalent of reverse correlation techniques in electrophysiology (e. g., Jones & Palmer, 1987; Ringach, Sapiro, & Shapley, 1997). Response classification has been employed most typically in estimating the spatial information use in a given task, or classification images; in this context, it is described as measuring the perceptual template of the observer (see the special issue of *Journal of Vision* introduced by Eckstein & Ahumada, 2002). Several studies have also assessed temporal information use with response classification, sometimes known as classification movies (e. g., Caspi, Beutter, & Eckstein, 2004; Ghose, 2006; Ludwig, Gilchrist, McSorley, & Baddeley, 2005; Neri & Heeger, 2002; Shimozaki, Chen, Abbey, & Eckstein, 2007).

In the current study, observers performed a cued yes/no contrast discrimination task over two possible locations (upper left and upper right, see Figure 1). The signal was a high-contrast Gabor pattern appearing at one of the two locations (on the left of Figure 1A) appearing on half the trials, with the other location having a lower-contrast 'pedestal' Gabor. The other half of the trials contained two pedestal Gabors, and observers judged upon the presence of the signal. Two 'standard' Gabors appeared in the upper center of the display (with the signal higher than the nonsignal pedestal in Figure 1A) as a reference for the observers. A dark square cue appeared at one location (left in Figure 1A) simultaneously with the stimulus indicating the probable location of the signal with 80% validity, when the signal was present. Thus, the overall breakdown of trial types (Figure 1B) was 40% valid signal present, 10% invalid signal present (cue opposite to signal location), and 50% signal absent.

The stimuli were presented in 'contrast noise' (Figure 2). Each trial had a stimulus duration of 272 ms, divided into 12 equal intervals (frames). On each frame, the peak contrast of each Gabor was varied randomly and independently around a mean peak contrast value representing the appropriate stimulus (signal or nonsignal pedestal). This gave the appearance of two 'flickering' Gabors at the two locations. The contrast noise was the basis of the response classification calculation, described schematically in Figure 3. First, the signal absent trials were pooled by the response outcomes, either the false alarm errors ('yes') or the correct rejections ('no'), with false alarms depicted in Figure 3. The contrast noise was averaged separately for each location (cued or uncued) and for each interval. The average is the classification number, which can be described as summarizing the total information used for that location and interval. This results in two classification number functions for the false alarm trials, one for the cued location and one for the uncued location, over the stimulus duration. Two other classification number functions (cued and uncued) were found for the correct rejection trials; the false alarm and correct rejection functions were then combined linearly (Ahumada, 2002; Murray, Bennett, & Sekuler, 2002), giving a single classification number function for both the cued and the uncued locations.

The main aim of this study was to compare the classification number functions for the cued and uncued locations. Figure 4 gives the predictions for strong versions of a parallel and a serial account of attention. From a previous study (Shimozaki et al., 2007), we would expect the overall form of the functions to rise and fall, with a positive skew (longer tail to the right). Also, we expect that the cue validity effect to be represented as less information being used at the uncued location (leading to lower-amplitude classification number functions), even for a parallel-noisy model. Thus, a difference in amplitude between cued and uncued locations does not necessarily imply a difference in temporal dynamics (this will be

shown in the Results and discussed further in the Discussion). This is analogous to stating that behavioral cueing effects on their own do not imply serial and/or limited capacity, as they can be predicted by parallel-noisy models (Eckstein et al., 2002; Shimozaki et al., 2003).

Central to the description of a serial attentional model is that, in a cueing task, the cued location is processed sooner than the uncued locations. This is consistent with limited capacity descriptions of attention that state that cued (attended) locations have speeded processing (Carrasco et al., 2004, 2006; Carrasco & McElree, 2001). Critically, a serial account of attention predicts a delay or shift of information use at the uncued location, compared to the cued location, whereas a parallel account of attention predicts no such delay. In terms of the classification number functions, scaling the uncued functions to the same amplitudes as the cued functions (shown on the bottom of Figure 4) predicts a difference in these functions for the serial model (lower left, Figure 4), and no difference for the parallel model (lower right, Figure 4). Thus, this study compared the cued functions to the scaled uncued functions to assess these predictions.

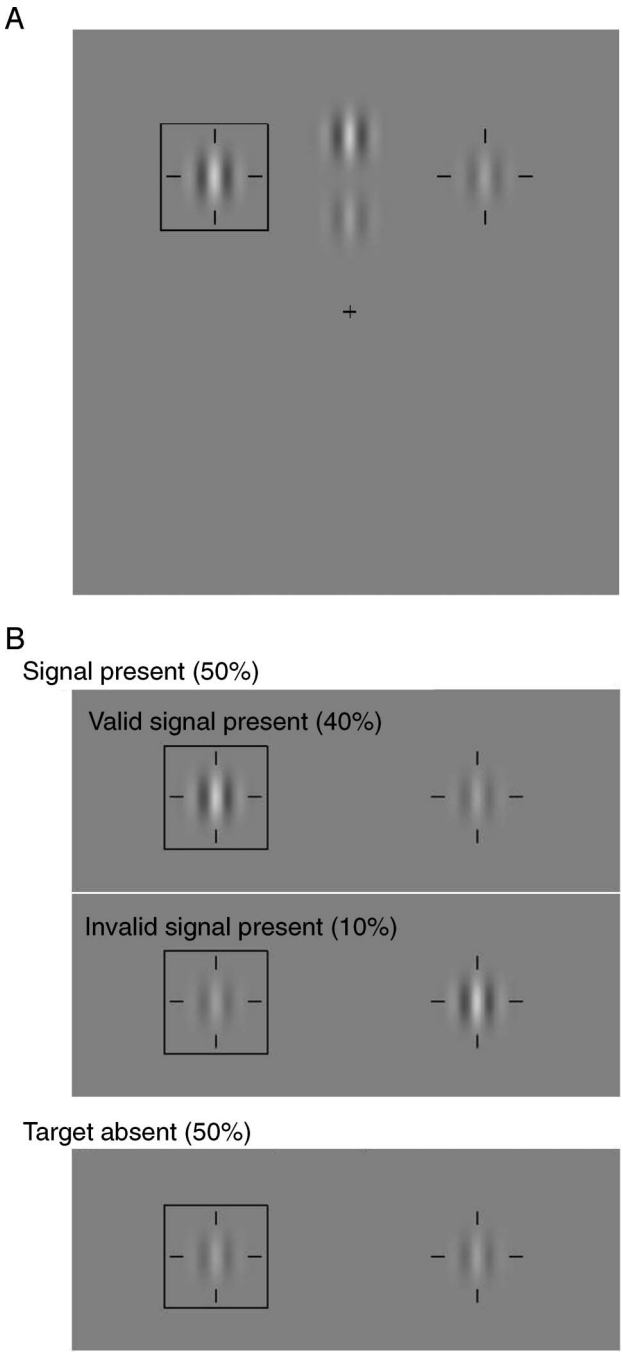

Figure 1. A. An example of the stimuli for the study. Observers performed a cued yes/no contrast discrimination task of Gabor patterns over 2 locations. A simultaneous cue had 80% validity when the signal was present. The figure depicts a valid signal present trial with the cue and signal on the left. Directly above the fixation cross, standard Gabor patches for the signal (upper patch) and the nonsignal pedestal (lower patch) were continuously displayed as a reference for the observer. Differences in contrast in this figure are larger than those used in the study. See the text for details. B. A summary of all trial types. Half the trials were signal present, and half the trials were signal absent. There were two types of signal present trials, valid and invalid, with the cue being 80% valid within the signal present trials. Thus, overall there were three trial types, valid signal present (top, 40% of all trials), invalid signal present (middle, 10% of all trials), and signal absent (bottom, 50% of all trials). For the purposes of this figure, the standards of the signal and nonsignal Gabors directly above the fixation cross are removed. Differences in contrast in this figure are larger than those used in the study.

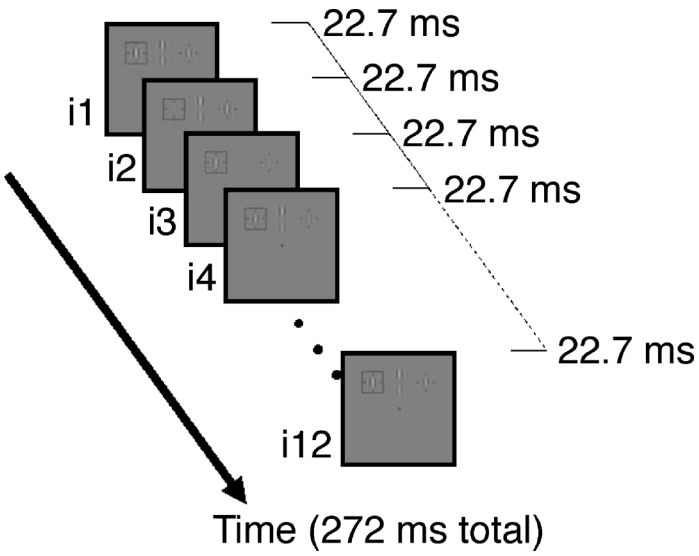

Figure 2. The contrast noise for each trial. Each trial had a stimulus duration of 272 ms, divided into 12 equal intervals (frames) of 22.7 ms each. The peak contrasts of the cued and uncued Gabor patches were perturbed randomly from interval to interval around the mean peak contrasts representing the stimuli (signal or nonsignal) for that trial. This had the appearance of a 'flickering' Gabor at each location.

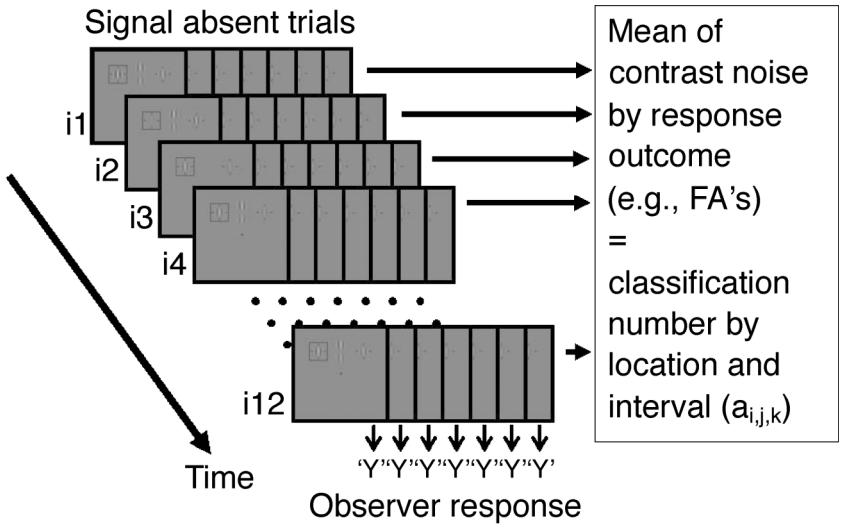

Figure 3. The calculation of the classification numbers. The figure depicts the calculation from the false alarms ('yes' observer responses on the signal absent trials). For each interval and location (cued or uncued), the mean of the contrast noise for the false alarm trials gave a classification number, resulting in two classification number functions (cued and uncued) through time for the false alarm trials.

Aside from the cued and scaled uncued comparisons, this study also assessed the stimulus durations leading to the peak amplitudes of the functions (the 'peak times'), after smoothing the functions with 3rd-degree polynomials. The serial model predicts a difference in the peak times, whereas the parallel model does not. Also, the results were compared to a representative parallel-noisy model for the cueing task, the weighted likelihood model. First, the behavioral response rates (hits, misses, corrections, and false alarms) were compared to the weighted likelihood model. Second, the integrals of the cued and uncued functions were compared to the predictions from an extension of the weighted likelihood model. In addition to the assumptions of the weighted likelihood model, the

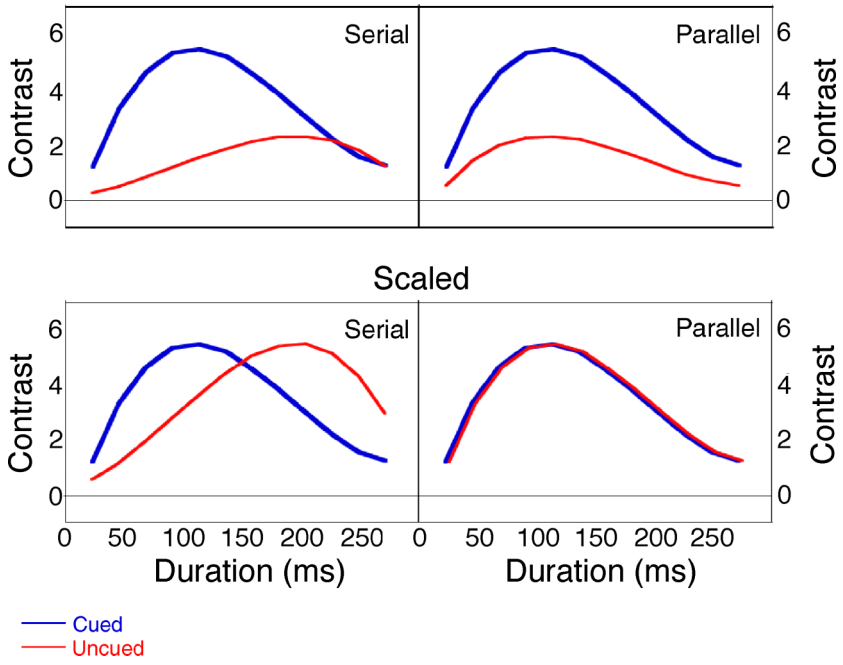

Figure 4. Predictions of the cued and uncued classification number functions for serial (left) and parallel (right) models of attention. The top figures represent the raw functions. The bottom figures represent the scaled functions in which the uncued classification number function amplitudes are scaled to match the amplitudes of the cued functions. The serial model predicts a shift or delay in the uncued function, whereas the parallel model does not. Predictions were generated from hypothesized representative 3rd-degree polynomial functions, similar to those employed to smooth the original classification number functions in this study.

extended model assumed a linear combination of information use across intervals, weighted by the smoothed classification number functions from the cued location. This comparison of integrals was performed as a method to assess the total amount of information use throughout the stimulus duration, both for the human observers and the weighted likelihood model.

A similar study by Shimozaki et al. (2007) performed a spatial and temporal response classification analysis over 8 intervals and a stimulus duration of 300 ms (37.5 ms/interval) in a cueing task with 8 locations (1 cued and 7 uncued) and a 100% valid cue. For the cued location, the attentional latency, in terms of the earliest evidence of information use at the cued location, was found for either the first (37.5 ms) or second (70.0 ms) interval. As the cue was 100% valid, information use at the uncued location was neither predicted nor found, and thus did not allow a comparison between the cued and uncued locations. The current study was designed specifically for this comparison with the response classification technique.

The current study might be seen as the temporal equivalent to a previous study assessing spatial information use, or perceptual templates, at cued and uncued locations in a cueing task with response classification (Eckstein et al., 2002). In Eckstein et al. (2002), as in the current study, there were two locations (cued and uncued) with 80% valid cues in the signal present trials. The results supported a parallel-noisy account over a limited capacity account. The amplitudes of the classification images at the cued locations were greater than those found at the uncued locations; however, when the amplitudes were matched, no differences were found between the shapes of the perceptual templates at the cued and uncued locations. This was consistent with predictions of an ideal Bayesian observer, and inconsistent with a 'tuning' limited capacity model that assumes that attention tunes the perceptual template at the cued location to an optimal shape (Carrasco, Williams, & Yeshurun, 2002; Golla, Ignashchenkova, Haarmeier, & Thier, 2004; Montagna, Pestilli, & Carrasco, 2009; Spitzer, Desimone, & Moran, 1988; Yeshurun & Carrasco, 1998, 1999).

Methods

4 observers with normal or corrected-to-normal acuity (AW, female, age 22 years; FB, female, age 22 years; LO, female, age 21 years; SS, male, age 45 years, author) performed a yes/no cued contrast discrimination task of a Gabor signal across two locations (see Figure 1). On half the trials (signal present), the signal appeared at one of the locations, with a nonsignal lower contrast 'pedestal' Gabor at the other location; on the other half of the trials (signal absent), the pedestal appeared at both locations. Observers made a yes/no judgment upon signal presence at either location. A square cue appeared simultaneously with the stimulus at one of the possible signal locations. For the signal present trials, the cue indicated the signal location with 80% validity. Thus, over all trials, 40% were valid signal present trials, 10% were invalid signal present trials, and 50% were signal absent trials (see Figure 1B). The order of the trial types, the location of the cue, and the location of the signal (on signal present trials) were randomized.

Stimuli were presented for 272 ms to minimize the effects of predictive saccades. Each Gabor was presented in 'contrast noise,' such that the peak contrast varied randomly (Gaussian-distributed) across 12 intervals or frames (22.7 ms each) around the mean contrast values that represented either the signal or the nonsignal pedestal (see Figure 2). This contrast noise formed the basis of the classification number analysis. For observers AW, FB, and LO, the standard deviation of the contrast noise was 14.1%. Due to SS's experience with psychophysical tasks, the task was made more difficult for him to approximately equate performance across observers, with a slightly smaller mean peak contrast for the signal (11.7% vs. 15.6%) and a slightly larger standard deviation for the contrast noise (15.6% vs. 14.1%).

The signal was a vertical Gabor pattern (1 cpd, 1 octave bandwidth, half-height, full width, 15.6% mean peak contrast) placed upon a (nonsignal) pedestal of 23.4% peak contrast. The signal could appear at two possible locations presented diagonally from a central fixation point, 5° upwards and either 5° left or 5° right of central fixation, giving a total eccentricity of 7.07°. The cue was a dark square cue (length = 4°, width = 4.2′, luminance = 0.77 cd/m^2), simultaneously and continuously displayed throughout the stimulus duration. A dark fixation cross was visible continuously in the center of the display (length = 0.5°, width = 4.2′, luminance = 0.77 cd/m^2), as well as four dark fiduciary 'tick marks' near each possible signal location (1.25° from the center of the stimulus) to reduce location uncertainty (length = 0.5°, width = 4.2′, luminance = 0.77 cd/m^2). Also, two copies of the signal and nonsignal pedestal Gabors were visible continuously 6.5° (signal) and 3.5° (pedestal) above the central fixation point as standard references for the observer.

Observers were informed of the cue validity, and observers were also trained and instructed to maintain fixation on the central cross throughout the stimulus duration. Each observer performed in approximately 20,000 trials across 16 sessions with 1250 trials in each session.

Stimuli were displayed using Matlab (The Mathworks, Inc., Natick, Massachusetts) and the Psychophysics toolbox (Brainard, 1997; Pelli, 1997) on a ViewSonic P227f monitor (39.1 cm × 29.3 cm, 1280 × pixels, 0.3052 mm/pixel) at 88 HZ with a viewing distance of 50 cm. The monitor was controlled by a Bits++ graphics card (Cambridge Research Systems, Cambridge, United Kingdom),

and luminance calibration was performed with the ColorCal colorimeter and software (Cambridge Research Systems, Cambridge, United Kingdom). The mean luminance of the display was 81.2 cd/m^2, and all stimuli were achromatic (gray, CIE coordinates, x = .284, y = .309).

Data analyses

Analyses of behavioral responses and the weighted likelihood model

The behavioral responses were characterized as the rates for each response outcome (hit and miss rates for valid signal trials, hit and miss rates for invalid signal trials, false alarm and correction rejection rates for signal absent trials). These rates were fit to the weighted likelihood model (Droll, Abbey, & Eckstein, 2009; Eckstein, Peterson, Pham, & Droll, 2009; Eckstein et al., 2002; Shimozaki et al., 2003), a parallel-noisy model of behavioral performance for cueing tasks (see Figure 5). This model is an extension of the Bayesian ideal observer for the task, and could be described generally as assessing how well (optimally) the observers use the cue validity in their judgments. Also, it provides an estimate of d' and bias (criterion) that accounts for decisions over multiple locations (e.g., Eckstein et al., 2000; Palmer, 1995; Palmer et al., 1993; Palmer et al., 2000; Verghese, 2001), as it falls under the class of 'parallel-noisy' models that predict set size effects (decreasing performance with increasing set size or number of items) based on parallel processing over increasingly noisier decisions. An important aspect of the weighted likelihood model is that it predicts a cueing effect when the cue validity is used optimally. As this is a parallel model, this implies that cueing effects, by themselves, do not indicate a serial effect of attention.

For each trial n, the weighted likelihood model starts with an input variable for each location j (cued or uncued), $x_{j,n}$. This input variable is assumed to be Gaussian-distributed, and assumed to be the sum of the internal representation of the mean contrast for that location and trial ($\alpha_{j,n}$), plus an error term ($\varepsilon_{j,n}$), such that

$$x_{j,n} = \alpha_{j,n} + \varepsilon_{j,n}. \quad (1)$$

The error term is the internal representation of the observer's total noise, and (assuming independence) is the sum of the overall added (external) contrast noise across intervals and the internal noise of the observer, or

$$\varepsilon_{j,n} = \varepsilon_{j,n,external} + \varepsilon_{j,n,internal}. \quad (2)$$

For each location, the model calculates the internal estimate of the posterior probability of signal presence (S_1) for each location j. First, the likelihood of signal presence ($l_{j,n}$) is calculated, which is the prior probability of the input variables at all locations, given signal presence at that location ($S_{1,j,n}$). For this task with two locations, the input variables comprise a two-element vector $\mathbf{x}_n$, where

$$\mathbf{x}_n = [x_{cued,n}, x_{uncued,n}], \quad (3)$$

and the likelihood may be expressed as

$$l_{j,n} = \mathrm{p}(\mathbf{x}_n|\mathrm{S}_{1,j,n}). \quad (4)$$

If we assume normalized Gaussian distributions ($\sigma = 1$) for x, with a mean of zero for the signal absent distribution and a mean of d' for the signal present distribution, we can define a probability density function $g(x)$ for both signal present and signal absent distributions, where

$$\mathrm{g}_0(x) = \frac{1}{\sqrt{2\pi}} e^{\left(-\frac{1}{2}x^2\right)}, \quad (5)$$

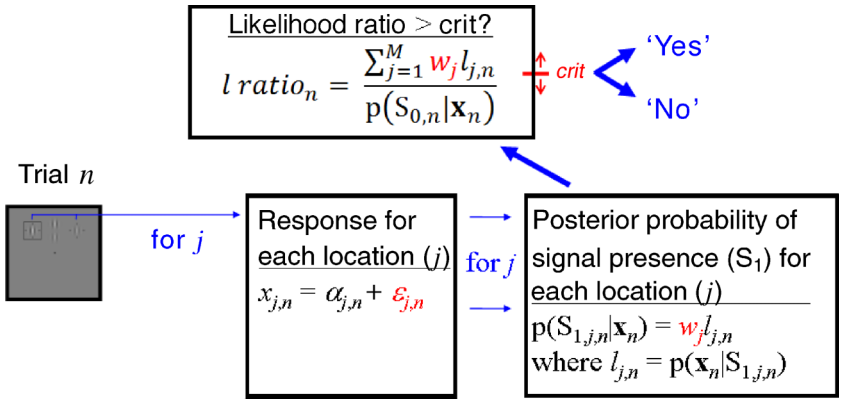

Figure 5. A schematic for the weighted likelihood model. One trial (n) is depicted with the 2 (cued and uncued) locations, starting with the stimulus on the left. The subscript j refers to location, with a total of M (= 2) locations. Items in red represent free parameters for the fits to the observers' response rates. See the text for details.

and

$$g_1(x) = \frac{1}{\sqrt{2\pi}} e^{\left(-\frac{1}{2}(x-d')^2\right)}, \quad (6)$$

with the subscripts 0 = signal absent, 1 = signal present, S_0 = the state of signal absence, and S_1 = the state of signal presence. For $p(\mathbf{x}_n|S_{1,j,n})$, we must consider the joint probability of signal presence at location j and signal absence at location $\neq j$. Therefore,

$$l_{j,n} = p(\mathbf{x}_n|S_{1,j,n}) = g_1(x_{j,n})g_0(x_{\neq j,n}). \quad (7)$$

Bayes' theorem is then applied to find the internal estimate of the posterior probability of signal presence for each location, $p(S_{1,j,n}|\mathbf{x}_n)$ by weighting the likelihoods by the internal estimate of the prior probability of signal presence at that location ($p(S_{1,j}) = w_j$), such that

$$p(S_{1,j,n}|\mathbf{x}_n) = p(S_{1,j})p(\mathbf{x}_n|S_{1,j,n}) = w_j l_{j,n}. \quad (8)$$

Note that the base rate of $p(\mathbf{x}_n)$ is not included in this formulation. Ideally the weights would represent the cue validity (i.e., $w_{cued} = 0.80$, $w_{uncued} = 0.20$); however, the human observer may diverge from these ideal weightings. Thus, the estimate of the human observer weights serves as an assessment of how well (or optimally) the observer could use the information provided by the cue validity.

The model then calculates the probability of signal presence given $\mathbf{x}$ over the probability of signal absence given $\mathbf{x}$, or the likelihood ratio, so that

$$l\ ratio_n = \frac{p(S_{1,n}|\mathbf{x}_n)}{p(S_{0,n}|\mathbf{x}_n).} \quad (9)$$

For $p(S_{1,j,n}|\mathbf{x}_n)$, we consider the probability of signal presence at the cued location or at the uncued location, so that

$$p(S_{1,n}|\mathbf{x}_n) = \sum_{j=1}^{M} p(S_{1,j,n}|\mathbf{x}_n) = \sum_{j=1}^{M} w_j l_{j,n}, \quad (10)$$

with M = number of locations = 2.

Thus, the likelihood ratio may be expressed as

$$l\ ratio_n = \frac{\sum_{j=1}^{M} w_j l_{j,n}}{p(S_{0,n}|\mathbf{x}_n)}. \quad (11)$$

For $p(S_{0,n}|\mathbf{x}_n)$, we must consider the probability of signal absence at the cued location and the uncued location; therefore,

$$\begin{aligned} p(S_{0,n}|\mathbf{x}_n) &= p(S_{0,cued,n}|x_{cued,n})p(S_{0,uncued,n}|x_{uncued,n}) \\ &= g_0(x_{cued,n})g_0(x_{uncued,n}). \end{aligned} \quad (12)$$

The likelihood ratio is compared to a criterion (*crit*); if the ratio is larger than the criterion, the model responds 'yes,' and if the ratio is below the criterion, the model responds 'no.' Thus, we may predict the behavioral response rates for the model for a given d', weight and criterion from the following cumulative probabilities Pr over all trials n:

$$valid\ hit\ rate = \Pr(l\ ratio_n > crit|S_{1,cued,n}, S_{0,uncued,n}), \quad (13)$$

$$invalid\ hit\ rate = \Pr(l\ ratio_n > crit|S_{0,cued,n}, S_{1,uncued,n}), \quad (14)$$

and

$$false\ alarm\ rate = \Pr(l\ ratio_n > crit|S_{0,cued,n}, S_{0,uncued,n}). \quad (15)$$

These weighted likelihood model predictions for the response rates were estimated through Monte Carlo simulations with 50,000 iterations (trials) for each d', criterion, and weight (Shimozaki et al., 2003). Then the best fits of these predicted response rates to the response rates of the human observers were found. The parts of Figure 5 in red indicate those parameters that were free to vary in the fits with the observer. These were the weights for the cued and uncued locations (w_j), the criterion (*crit*), and the internal representation of the total noise ($\varepsilon_{j,n}$). The last item ($\varepsilon_{j,n}$) was expressed as the overall d' for the observer. Also, fits were performed with a fixed optimal weight of 0.80 and d' and the criterion as free parameters.

To change the weighted likelihood model to the ideal observer, the input variable $x_{j,n}$ is the result of a cross-correlation (linear operator) of an ideal template with the stimulus; in white Gaussian spatial noise, the ideal template is the same as the signal. The weight for the likelihood for the cued location (w_{cued}) is the probability of cue appearance at the cued location, or the cue validity (0.80). The criterion is the ratio of the probabilities for target presence and target absence, which was 1.0 for this study. Finally, there would be no internal noise, and therefore $\varepsilon_{j,n} = \varepsilon_{j,n,external}$.

The criteria are presented as their logarithms, so that log (*crit*) = 0 represents unbiased decisions.

Analyses of classification numbers

As discussed in the Introduction, a classification number was calculated for each location (cued and uncued) and each interval (12 total intervals). Each classification number may be described as summarizing the amount information used during that interval, resulting in two classification number functions, one cued and one uncued, describing the information use throughout the stimulus duration.

For the classification numbers, trials were first pooled by the response outcomes for the signal absent trials (i.e., by either false alarms or correct rejections) for each observer (see Figure 3). Figure 3 demonstrates an example of pooling by false alarms (signal absent trials in which the observer responds 'yes'). A classification number (a) was calculated as the mean of the added contrast noise ($\varepsilon_{external}$) across all trials (N), taken separately for each interval (i), each location (j, where j = *cued* or *uncued*), and each outcome (k, where k = *false alarm* or *correct rejection*), as follows:

$$a_{i,j,k} = \frac{\sum_{n=1}^{N_{i,j,k}} \varepsilon_{i,j,k,n,external}}{N_{i,j,k}}. \quad (16)$$

This gave four classification number functions through time for each observer: false alarm-cued, false alarm-uncued, correct rejection-cued, and correct rejection-uncued. The classification numbers for cued and uncued locations were combined across the false alarms and correct rejections (Ahumada, 2002; Murray et al., 2002; Shimozaki et al., 2007), so that

$$a_{i,j} = a_{i,j,false\ alarm} + a_{i,j,correct\ rejection}. \quad (17)$$

This gave two classification number functions through time for each observer, one for the cued location and one for the uncued location. As the classification number calculations were based on all the signal absent trials, the number of trials for these calculations was approximately half the total number of trials, or about 10,000 trials (AW = 9779, FB = 9779, LO = 9804, SS = 9832).

Comparisons between the overall classification number functions were performed with the Hotelling T^2 statistic (Harris, 1985), which is the multivariate generalization of the univariate t statistic, and analogous to the t statistic has two forms, one-sample and two-sample (see Appendix A). The one-sample Hotelling T^2 statistic with a diagonal covariance matrix $\mathbf{K}$ (i.e., all zero correlations) is distributed as a χ^2 statistic, and it was found that the covariance matrices for the sample classification number functions were nearly diagonal (see Appendix A). Therefore, for differences between the sample classification number functions and hypothesized models (with q = number of free parameters), the one-sample Hotelling T^2 statistics were evaluated as χ^2 statistics for the model, and $df = p - q$.

To compare the durations giving the maximal amplitudes (peak times) for the cued and uncued functions, further analyses were undertaken to fit the classification number functions to log-Gaussian, Poisson, and polynomial functions. Also, the results of these fits were assessed to estimate the integrals of these functions through time. Finally, the fits were used as interval weights to compare the observed estimated integrals to predictions from an extended weighted likelihood model that included a weighted linear summation across intervals.

Results

Behavioral results

Figure 6 and Table B1 in Appendix B summarize the behavioral response results for the four observers. As shown by the first column of Table B1a, the overall proportion correct across observers was relatively consistent, ranging from 0.737 to 0.792. The last three columns of Table B1a and Figure 6 give the response rates for valid hits ('yes' responses on valid signal trials), invalid hits ('yes' responses on invalid signal trials), and false alarms ('yes' responses for signal absent trials). Hits rates were

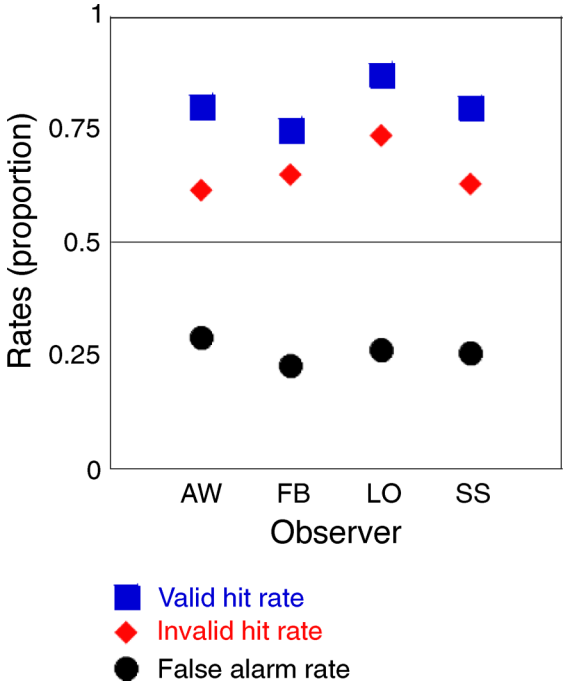

Figure 6. The behavioral response rates for each observer. Valid hit rate = blue squares. Invalid hit rate = red diamonds. False alarm rate = black circles.

Table 1a

Observer	d'	Weight, cued location (w_{cued})	log(criterion)	w_{uncued}/w_{cued}
AW	1.50	0.81	−0.18	0.235
FB	1.60	0.67	0.05	0.492
LO	1.92	0.81	−0.42	0.235
SS	1.61	0.80	−0.13	0.250

Table 1b

Observer	d'	Weight, cued location (w_{cued})	log(criterion)	$\chi^2(1)$	p-value	Sig.
AW	1.50	0.80	−0.17	1.141	0.2854	
FB	1.60	0.80	0.01	60.504	0.0000	*
LO	1.92	0.80	−0.41	0.437	0.5085	
SS	1.61	0.80	−0.13	0.291	0.5895	

Table 1. Fits of the behavioral performance to the weighted likelihood model (Figure 5). 1a. Fits with d', weight, and criterion (expressed as log criterion) as free parameters. 1b. Fits with d' and criterion as free parameters, and the weight fixed to the optimal value of 0.80 (the cue validity). Fits were assessed with χ^2 and degrees of freedom = 3 − 2 free parameters = 1. *Note*: * = $p < .05$.

larger than 0.50, and false alarm rates were less than 0.50, indicating better than chance performance in the yes/no task. Also, the valid hit rates were greater than the invalid hit rates, indicating the use of the cue by the observers, or the cue validity effect. Table B1b summarizes cue validity effect as the difference between the valid hit rate and invalid hit rate (Eckstein et al., 2002; Shimozaki et al., 2003). Each observer showed a positive cue validity effect, ranging from 0.101 to 0.186, and the χ^2 results indicated these cueing effects were highly significant.

Table 1 summarizes the fits of the rates of the behavioral responses to the weighted likelihood model, as assessed by χ^2 goodness of fit statistics. As mentioned earlier, the weighted likelihood model is a parallel model of performance that also gives an estimate of the observed cue validity effect relative to an optimal Bayesian decision rule. Also, it provides a measure of d' and bias that accounts for multiple locations (Eckstein et al., 2000; Palmer, 1995; Palmer et al., 1993, 2000; Verghese, 2001). Table 1a gives the weighted likelihood fits with the cued location weight (w_{cued}) as a free parameter, with the optimal cued weight equaling the actual cue validity of 0.80 (and therefore 1.00 − 0.80 = 0.20 at the uncued location). The free parameters (d', w_{cued}, log(criterion)) equal the total degrees of freedom (3, for each trial type); thus, no χ^2 statistics are presented. As shown in Table 1a, these estimated weights for each observer indeed were near the optimal weight of 0.80, except for FB, whose weight was less than optimal (0.67). For w_{unued}/w_{cued}, the optimal weight of 0.80 corresponds to a ratio of 0.250 = $(1.0 - w_{cued})/w_{cued}$ = (1.0 − 0.8)/0.8.

Table 1b gives the fits to the weighted likelihood model for a fixed optimal cued location weight (w_{cued}) of 0.80. This gave a fit with two free parameters (d', criterion) and thus one degree of freedom for the χ^2 statistic (3 total df − 2). As might be expected from Table 1a, the fits to the optimally weighted model were not significantly different (indicating nearly optimal weighting) for all observers except for FB. Thus, the observers' performances (except FB) were fit well to a parallel model with an optimal weighting of cued information.

The d's were relatively consistent across observers, ranging from 1.50 to 1.92, as would be expected from the relatively consistent results for proportion correct (Table B1a, column 1). Generally across observers the log-criteria were slightly negative, indicating a slight bias to respond 'yes.'

Classification number functions

Figure 7 summarizes the classification number functions for cued and uncued locations across observers; tables for these functions may be found in Appendix C, Table C1. Blue indicates the cued location functions, and red indicates the uncued location functions. Overall, the functions rise to a peak and then fall off at the end of the stimulus duration. Also, the cued functions appear to have substantially larger amplitudes. Hotelling T^2 statistics (Table C2) confirmed that all functions (across intervals) were significantly different from zero (one-sample Hotelling T^2, Table C2a), and that all the cued functions were significantly greater than the uncued functions (two-sample Hotelling T^2, Table C2b).

Each interval was assessed for significant differences from zero with single-sample t-tests, corrected for multiple comparisons across the 12 intervals with the Simes-Hochberg method; this method is similar to the Bonferroni correction, but is considered more appropriate given the conservative characteristics of the Bonferroni correction (Hochberg, 1988; Simes, 1986). Significant differences from zero are indicated in Figure 7 as filled circles, and are also summarized in Table C1. A significant difference from zero would indicate a significant use of information for that interval at the given location. As shown in Figure 7, there was evidence of significant information use for both

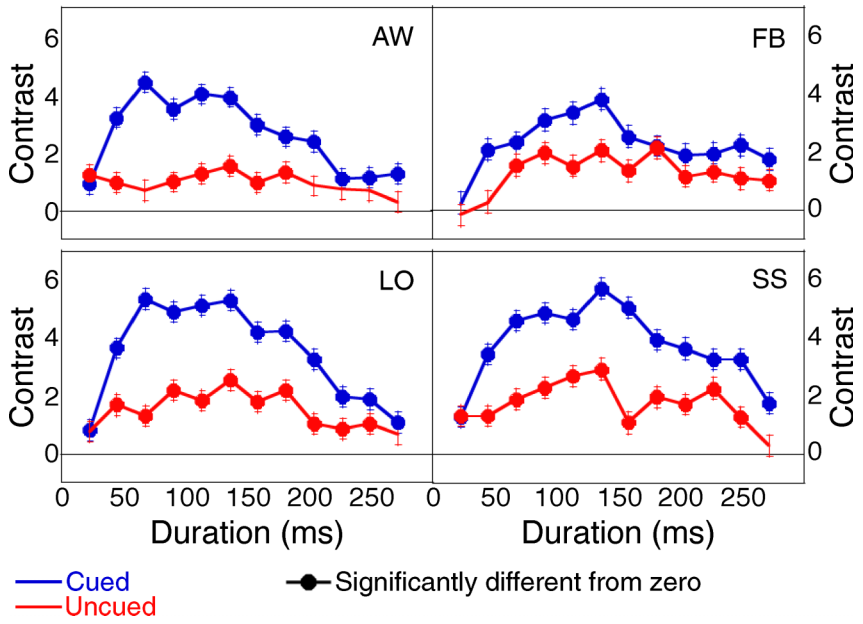

Figure 7. The classification number functions for each observer. Cued = blue. Uncued = red. The filled circles indicate significant differences from zero, as assessed by single-sample *t*-tests, adjusted for multiple comparisons by the Simes-Hochberg method. Error bars represent standard errors of the mean.

cued and uncued locations throughout the stimulus duration. The first interval with significant information use might be considered an estimate of the latency for this task. By this definition, the latency for the cued location was the first interval (22.7 ms) for all observers except FB, who had a latency of the second interval (45.3 ms). These results were consistent with the results from Shimozaki et al. (2007), which found evidence of the first use of information at cued locations at 37.5 ms (2 observers) to 75 ms (1 observer). For the uncued location, these estimates of latency were slightly later, the first interval (22.7 ms) for AW and SS, the second interval (45.3 ms) for LO, and the third interval (68.0 ms) for FB.

Each interval was also assessed for differences between the cued and uncued functions by independent two-sample *t*-tests, adjusted for multiple corrections with the Simes-Hochberg method. These results are also summarized in Table C1. For all observers, the cued and uncued functions differed significantly by the 2nd interval (45.3 ms); for all observers except FB, the cued and uncued functions differed significantly interval-by-interval throughout most of the stimulus duration (AW: intervals 2–7,9; LO: intervals 2–9; SS: intervals 2–9,11,12). FB had fewer intervals with significant cued vs. uncued differences (intervals 2, 5, and 6), related to the higher amplitude of her uncued function relative to her cued function.

The latency estimates from the first interval that was significantly different from zero seems to suggest a slight delay for the uncued latencies. Also, the results comparing the cued and uncued functions (overall and interval-by-interval) indicate higher amplitudes for the cued functions. However, caution should be taken in using these comparisons as indications of a difference in temporal dynamics at the cued and uncued locations. As shown later, a parallel-noisy model (a simple extension of the weighted likelihood model) predicted equivalent differences in amplitudes. This finding is analogous to the behavioral cueing effects predicted by the weighted likelihood model (Table 1; Eckstein et al., 2002; Shimozaki et al., 2003), in that differences between cued and uncued locations were predicted by a parallel-noisy model. Also, the expected lower amplitudes for the uncued functions would necessitate that the first evidence of significant information use (differences from zero) would be later for the uncued functions, given the nearly equivalent variances for the cued and uncued functions (see Table C1). This point will be discussed further in the Discussion.

Figure 8 gives the cued functions (in blue, and the same as in Figure 7) compared to the uncued functions with amplitudes scaled to provide the best match to the cued functions. The goodness of fits of the matches were assessed with two-sample Hotelling T^2 statistics (Table 2). As expected from the interval-by-interval comparisons of the cued vs. uncued functions, FB had the largest scale factor of 0.57. The cued and the scaled uncued functions could not be distinguished statistically from each other, except for SS. For SS, a posthoc analysis was performed comparing the cued and uncued functions for each interval using independent two-sample *t*-tests, corrected for multiple corrections by the Simes-Hochberg method. It was found that the two functions differed only in the 7th interval at 158.7 ms ($t(19622) = 3.155$, p(uncorrected) = 0.0016). Thus, for three observers the comparison of the cued and the scaled uncued functions found no evidence

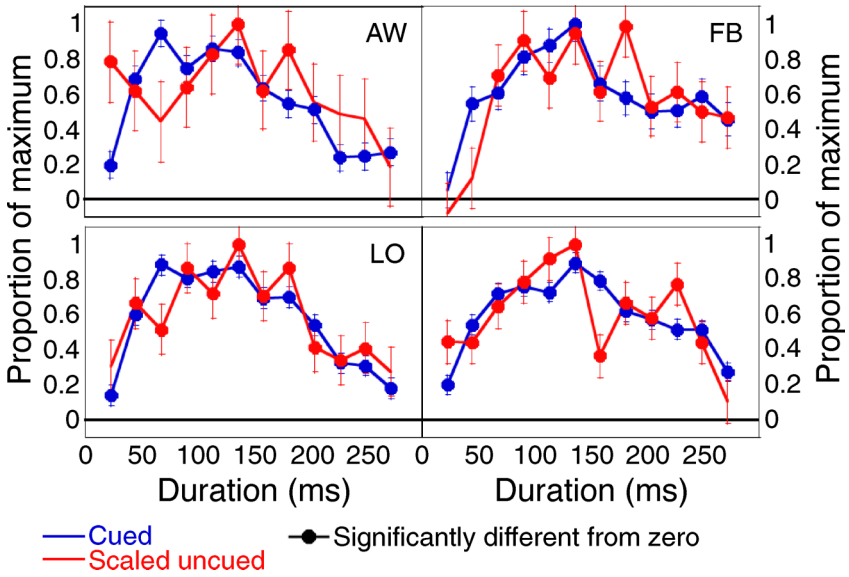

Figure 8. The classification number functions for each observer with the scaled uncued functions. The uncued location function amplitudes were scaled to give the best fit to the cued location functions (as assessed by two-sample Hotelling T^2). Cued = blue, and are the same as Figure 7. Scaled uncued = red. The filled circles indicate significant differences from zero, as assessed by single-sample *t*-tests, adjusted for multiple comparisons by the Simes-Hochberg method. Error bars represent standard errors of the mean.

of a difference, which does not favor a strong serial hypothesis. Also, the results of SS do not appear to suggest a shift in the functions in time, and thus does not appear to be congruent with the predictions from a serial model. Rather, there appears to be a 'dip' in the uncued function at an intermediate stimulus duration. This dip differs from the other observers, and there appears to be no obvious explanation.

Peak times and integrals of the classification number functions

Attempts were made to fit the classification number functions to various functions to 'smooth' the likely interval-to-interval noise in the original functions. These smoothed functions were then employed to estimate the durations giving the maximum amplitudes (peak times) of the original functions, as well as their integrals. Two functions that generally have positive skew (longer tails to the right) were attempted initially, log-Gaussian and Poisson (see Appendix D). Neither function provided adequate fits (see Table D2), particularly for the cued functions, and thus a more general fit to polynomial functions was attempted. Functions of time (t) from quadratic (2^{nd}) to quartic (4^{th}) degree were considered, such that

$$f(t) = c_0 + c_1 t + c_2 t^2 + c_3 t^3 + c_4 t^4, \quad (18)$$

with $c_4 = 0$ for the 3^{rd}-degree polynomial, and $c_3 = c_4 = 0$ for the 2^{nd}-degree polynomial. Fits were evaluated with one-sample Hotelling T^2 statistics, evaluated as χ^2's and with degrees of freedom = 12 − number of free parameters. It was found that no 4th-degree polynomial significantly improved the fit compared to the 3rd-degree polynomial (Hotelling T^2 difference = 0.04 to 2.94; p = 0.6548 to 0.0863). Thus, only the 3^{rd}-degree polynomial fits are presented, with the following format:

$$f(t) = c_0 + c_1 t + c_2 t^2 + c_3 t^3. \quad (19)$$

Figure 9 presents the data fits to the 3^{rd}-degree polynomials, and Table D1 in Appendix D summarizes

Observer	Scale	Hotelling T^2	df_2	F(12,df_2)	p-value	Sig.
AW	0.33	14.92	19545	1.243	0.2462	
FB	0.57	10.94	19545	0.911	0.5344	
LO	0.42	11.52	19595	0.960	0.4854	
SS	0.46	22.43	19651	1.869	0.0331	*

Table 2. Tests for differences between the cued and scaled uncued functions for each observer. The scaled uncued functions were found by matching the amplitudes of the uncued functions to provide the best fit to the cued functions, as assessed by two-sample Hotelling T^2 statistics. *Note*: * = $p < .05$.

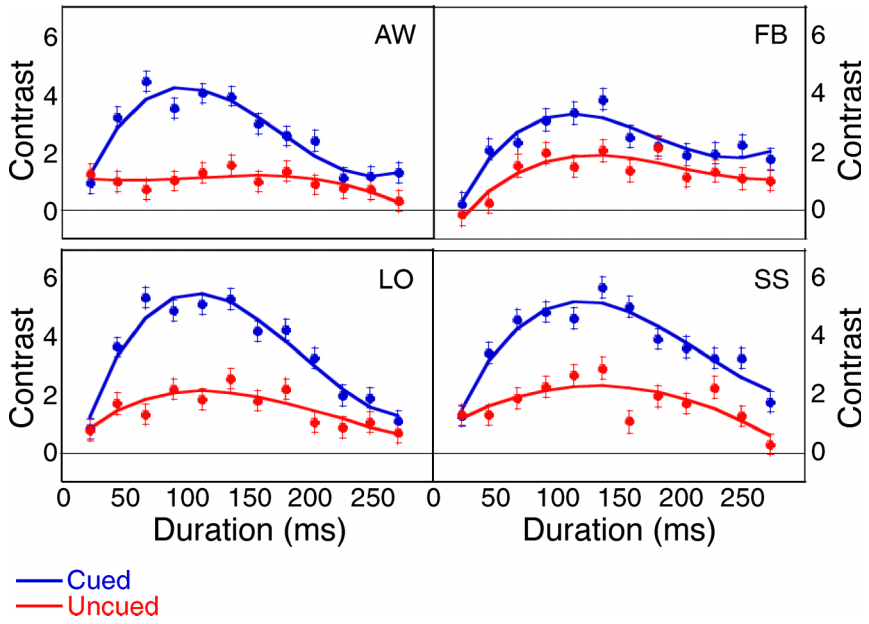

Figure 9. The 3rd-degree polynomial fits to the classification number functions for each observer. Cued = blue. Uncued = red. The small filled circles represent the original data, also presented in Figure 7.

the one-sample Hotelling T^2 statistics, evaluated as χ^2's and with degrees of freedom = 12 − 4 = 8. Also, Table D1 lists the fitted coefficients for the fits (c_0 to c_3), with time (t) in seconds. Except for the uncued data for SS, no significant differences were found between the data and the fitted polynomial models, indicating relatively good fits. As mentioned earlier, the data for SS at the uncued location had a 'dip' at the 7th interval (158.7 ms), which led to the poor fits to both the 3rd-degree and 4th-degree polynomial functions (4th-degree fit: Hotelling $T^2 = 19.89$, degrees of freedom = 7, $p = 0.0058$).

These polynomial fits were employed to assess the peak times for the cued and uncued functions. Standard errors of the peak times were estimated through a technique known as 'Monte Carlo resampling' (Efron & Tibshirani, 1993), which is related to bootstrapping. The classification number functions were resampled iteratively by using the values from the 3rd-degree polynomial fits, and then perturbing those values assuming Gaussian distributions with the same standard errors as the observed classification numbers. These resampled classification number functions were then refit to new 3rd-degree polynomials with χ^2 goodness-of-fits, and the peak times were found for the refit functions; standard errors were computed across iterations (50,000 for each peak time). The peak times (from the fitted polynomials) and the estimated standard errors are presented in Table 3. Also, Table 3 summarizes the comparisons of the cued and uncued peak times for each observer, assessed as independent two-sample t-tests. The cued peak times tended to be slightly less than the uncued peak times. However, the estimated standard errors for the uncued peak times were larger than those for the cued peak times; this was due to the lower-amplitude (i.e., 'flatter') uncued functions, leading to more uncertainty in the estimated peak times. This was particularly true for AW, who had a distinctly flat function

Observer		Peak time (ms)	Std. Err.	t	p-value	Sig.
AW	cued	99	3.24	0.825	0.4092	
	uncued	159	72.62			
FB	cued	112	6.14	0.775	0.4386	
	uncued	128	19.72			
LO	cued	109	3.16	0.453	0.6503	
	uncued	115	12.85			
SS	cued	120	5.23	0.654	0.5132	
	uncued	133	19.18			

Table 3. Estimates of the durations giving the maximal values (peak times). Estimates were based upon the 3rd-degree polynomial fits to the classification number functions (Table D1), and standard error estimates were based on resampling methods (see the text for details). Differences in the cued and uncued peak times were assessed with independent two-sample t-tests. *Note*: * = $p < .05$.

for the uncued location, and thus a rather large estimated standard error (72.6 ms). The result is that no significant differences were found between the peak times of the cued and uncued functions for any observer, arguing against a strong serial attentional hypothesis.

As each individual classification number for each interval might be interpreted as the information use for that interval, the integral of the classification number functions might be interpreted as the overall information use throughout the stimulus duration. Table 4 presents the integrals of the fitted uncued and cued functions (3rd-degree polynomials), with the standard errors calculated with the same method as the peak times (resampling based on the classification number standard errors and refitting with 3rd-degree polynomials with χ^2 goodness-of-fits over 50,000 iterations). The cued function integrals were significantly greater than the uncued function integrals, as assessed with independent two-sample *t*-tests, with ratios (uncued/cued) ranging from 0.396 (for LO) to 0.545 (for FB).

Comparison of classification number functions to an extended weighted likelihood model

A posthoc question that arises from the previous results is how the relative weightings for cued and uncued locations predicted from the weighted likelihood model might be reflected in the observed classification number functions. The relative weightings from the weighted likelihood fits (w_{uncued}/w_{cued}, from Table 1a) optimally should be (1.0 − 0.8)/0.8 = 0.25, and ranged from 0.235 (for AW and LO) to 0.492 (for FB). However, the scaling factors equalizing amplitudes across the cued and uncued classification number functions ranged from 0.33 (for AW) to 0.57 (for FB); also, the relative integrals from Table 4 ranged from 0.396 (for LO) to 0.545 (for FB). Thus, the general order across observers seem to correspond across these measures, with AW having the lowest and FB having the highest values; however, the relative weightings predicted by the weighted likelihood model seem lower than those expected from both the scaling factors and the relative integrals. However, we would not necessarily expect to find a linear relationship between the weights predicted from weighted likelihood and the characteristics of the classification number functions. One issue is that behavioral cueing effects (assessed as valid hit rate − invalid hit rate) predicted by the weighted likelihood model depends upon d', with small cueing effects predicted at both low and high d's (Shimozaki et al., 2003). Also, there would be differences in cueing effects based upon different criteria in the weighted likelihood model; consider the case in which the observer is completely biased to always respond 'yes' or 'no', which clearly would lead to no observable cueing effects. For these reasons, a final analysis was undertaken to predict the relative relationship between the weights from the weighted likelihood model and cued and uncued classification number functions, including the relative integral values for the cued and uncued functions, with an extension of the weighted likelihood model presented earlier (Figure 5).

This extension (Figure 10) is equivalent to the weighted likelihood model, with the exception that the input variable ($x_{j,n}$ for a given location *j, uncued* or *cued,* and trial *n*) is the result of the sum of weighted responses ($y_{i,j,n}$) across intervals (i), with the total number of intervals = H = 12. Each unweighted response is the internal representation for the contrast for a particular location j and trial n ($\alpha_{j,n}$), added to the internal representation of the total noise for that location *j,* trial *n,* and interval i ($\varepsilon_{i,j,n}$), with

$$\varepsilon_{i,j,n} = \varepsilon_{i,j,n,external} + \varepsilon_{i,j,n,internal}, \quad (20)$$

This equation is equivalent to Equation 2, except for the inclusion of the noise for each interval i.

This response is then weighted by the classification number for that interval i at the cued location, as given by the 3rd-degree polynomial fits described above ($a_{i,cued}$). Thus, the weighted internal response

$$y_{i,j,n} = a_{i,cued}(\alpha_{j,n} + \varepsilon_{i,j,n}), \quad (21)$$

Observer		Integral	Std. Err.	*t*	*p*-value	Sig.	Ratio, uncued/cued
AW	cued	0.687	0.029	10.283	0.0000	*	0.396
	uncued	0.272	0.029				
FB	cued	0.583	0.031	6.082	0.0000	*	0.545
	uncued	0.318	0.031				
LO	cued	0.921	0.029	12.481	0.0000	*	0.438
	uncued	0.403	0.029				
SS	cued	1.003	0.029	12.605	0.0000	*	0.478
	uncued	0.479	0.030				

Table 4. Estimates of the integrals of the classification number functions. Estimates were based upon the 3rd-degree polynomial fits to the classification number functions (Table D1), and standard error estimates were based on resampling methods (see the text for details). Differences in the cued and uncued integrals were assessed with independent two-sample *t*-tests. *Note*: * = $p < .05$.

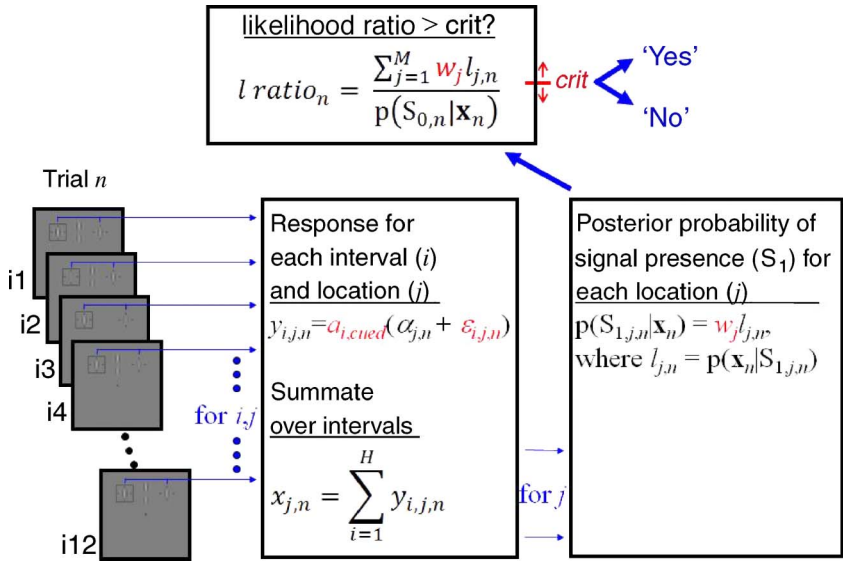

Figure 10. A schematic for the extended weighted likelihood model. This model assumes a linear summation across intervals (i), weighted by the classification number function at the cued location ($a_{i,cued}$). After the weighted linear summation, this model is the same as the weighted likelihood model (Figure 5). One trial (n) is depicted, starting with the stimulus and the intervals (i = 1 to 12) on the left. The items in red were determined by the observers' performance or cued classification number function. See the text for details.

and the input variable for each location j and trial n is the sum of the weighted responses across the intervals, or

$$x_{j,n} = \sum_{t=1}^{H} y_{i,j,n}. \quad (22)$$

From this point the extended model is the same as the weighted likelihood model (see Methods).

In Figure 10, those items in red were determined by the individual observers' performance or classification numbers. The weights for the intervals ($a_{j,cued}$) were determined by the observers' classification numbers for the cued location, as derived from the 3rd-degree polynomial fits. The internal representation of the total noise ($\varepsilon_{i,j,n}$) was determined so that the sensitivity for the extended model (d') matched that of the observers' fits to the

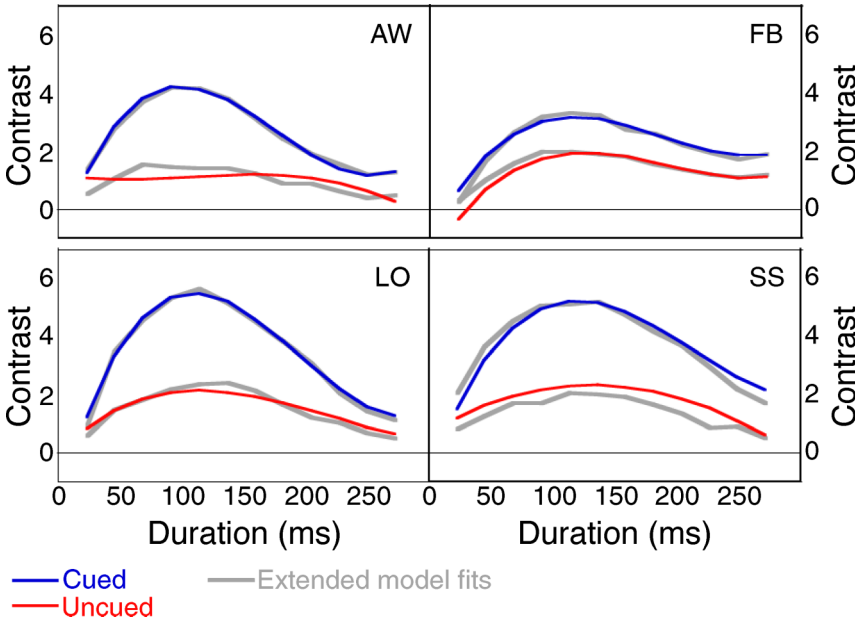

Figure 11. The predictions of the classification number functions from the extended weighted likelihood model (Figure 10). Cued 3rd-degree polynomial fit = blue, and also shown in Figure 9. Uncued 3rd-degree polynomial fit = red, and also shown in Figure 9. Predictions from the extended weighted likelihood model = gray.

Observer		Hotelling T^2	df_2	$F(12,df_2)$	p-value	Sig.
AW	uncued	0.872	19595	0.073	0.9999	
FB	uncued	1.597	19545	0.133	0.9998	
LO	uncued	3.026	19545	0.252	0.9954	
SS	uncued	16.877	19651	1.406	0.1548	

Table 5. Fits of the predicted classification number functions from the extended weighted likelihood model to the 3rd-degree polynomial functions for the uncued locations (Table D1). The fits were evaluated with two-sample Hotelling T^2 statistics using the covariance matrices from the original classification number functions. *Note*: * = $p < .05$.

weighted likelihood model presented earlier (Table 1a). The weights for the cued and uncued locations (w_j) and the criteria (*crit*) were also determined by the observers' fits to the weighted likelihood model. Thus, the extended model was completely determined and had no free parameters. Also, the observers' use of information at the uncued location was not represented, except as the difference in weights at the cued and uncued locations for the fitted weighted likelihood model (w_j). The predicted classification number functions from the extended model were found with Monte Carlo simulations with 50,000 trials for each observer.

Table E1 in Appendix E summarizes the fits of the behavioral response rates (i.e., valid hit, valid miss, invalid hit, invalid miss, false alarm, and correct rejection rates) from the simulations of the extended model with the observed response rates from each observer. The fits were good, with no significant differences; this was expected, as the extended model was designed to have the same performance as the weighted likelihood model (Table 1a), which in turn was matched to the observer response rates.

Figure 11, Table E2 (Appendix E) and Table 5 summarize the fits of the extended model predictions of the classification number functions to the original 3rd-degree polynomials. For these analyses, the cued functions for the extended model and the polynomials were matched to give the best fits. Figure 11 presents the same 3rd-degree polynomial fits shown in Figure 8, with cued in blue and uncued in red, and presents the extended model fits in gray. The amplitudes for the uncued functions were lower than those for the cued locations. This is expected from the difference in weights at the cued and uncued locations in the extended model, and is the representation of the cueing effect for the classification number functions. Note that this difference is predicted from a parallel-noisy model, analogous to cueing effects for behavioral responses (Table 1; Eckstein et al., 2002; Shimozaki et al., 2003). This finding highlights the point that cueing effects in cueing tasks do not necessarily indicate a serial, limited capacity attentional mechanism.

Table E2 summarizes the overall fits of the cued functions, assessed as two-sample Hotelling T^2 tests with the covariance matrices from the original data. The fits were good, which was not necessarily surprising, as the interval weights for the extended model did come from the cued location functions. However, it suggests that any nonlinear transformation of the extended model (i.e., the calculation of the likelihoods) did not have much relative effect from interval to interval on the resulting classification number functions.

The main goal of the extended model simulations was to predict the uncued location functions from the extended model. Tables 5 and 6 present the results of these predictions for the extended model against the uncued 3rd-degree polynomial fits (also shown in Figure 11). Table 5 gives the overall fits for the uncued functions, assessed as two-sample Hotelling T^2 tests with the covariance matrices from the original data. There were no significant differences for any observer, and the fits were good for all observers except SS, whose predicted uncued function was somewhat less than the 3rd-degree polynomial fits.

Table 6 presents the predicted integrals for the uncued functions from the extended model, compared with the uncued integrals from the 3rd-degree polynomial fits (also

Observer	3rd -degree polynomial uncued integral	Std. Err.	Extended weighted likelihood uncued integral	Std. Err.	t	p-value	Sig.
AW	0.272	0.029	0.260	0.036	0.248	0.8040	
FB	0.318	0.031	0.404	0.038	1.765	0.0775	
LO	0.403	0.029	0.362	0.039	0.841	0.4001	
SS	0.479	0.030	0.379	0.038	2.102	0.0355	*

Table 6. The predicted integrals for the uncued classification number functions from the extended weighted likelihood model. The standard error estimates were based on resampling methods (see the text for details). The integrals from the 3rd-degree polynomial fits (found in Table 4) also appear in this table for comparison. The differences in the predicted integrals and estimated integrals from the 3rd-degree polynomial fits were assessed with independent two-sample t-tests. *Note*: * = $p < .05$.

presented in Table 4). The standard errors for the integrals from the extended model were found with the same basic method as before. The predicted values for the classification numbers from the extended model were resampled with the standard errors from the original data; then these values were fitted with 3rd-degree polynomials with χ^2 goodness-of-fits over 50,000 iterations. Independent two-sample *t*-tests found no significant differences between the extended model and the original 3rd-degree polynomial fits, except for SS, which found that the extended model predictions were significantly smaller. The significant results for SS, however, likely were affected by the 'dip' at 158.7 ms that led to a poor fit to the original 3rd-degree polynomial (Table D1 and Figure 9). In summary, over both sets of results (Hotelling T^2's and integrals) the extended weighted likelihood model of weighted responses across intervals gave relatively good predictions for the uncued classification number functions, and therefore the relative differences between the cued and uncued functions. In other words, the total information use throughout the stimulus duration at the cued and uncued locations were predicted reasonably well with the extended weighted likelihood model.

Discussion

The temporal dynamics of information use was compared at the cued and uncued locations in a cueing task employing the response classification technique. A serial model of attention predicts a shift or delay of information use at the uncued location, compared to the cued location, whereas a parallel model predicts no such delay. The results show no significant evidence of a shift. Generally, the cued classification number functions did not differ from the uncued functions, scaled to the equivalent amplitudes; the exception was a 'dip' (not a shift) for the uncued function of SS. Also, the durations giving the peak amplitudes (the peak times), estimated from smoothed classification number functions, did not significantly differ between the cued and uncued functions. Finally, the observers' results were generally well fit to a representative parallel-noisy model, the weighted likelihood model. The behavioral response rates were relatively consistent with the optimal weighting predictions of the weighted likelihood model, and the relative integrals of the cued and uncued classification number functions were generally consistent with an extended weighted likelihood model assuming a weighted linear summation across intervals. As the parallel account is essentially the null hypothesis, some caution is necessary in the conclusions made from this study. However, over all the analyses (scaled classification number functions, peak times, fits to the parallel-noisy model), it seems that the data generally favor the parallel account.

It should be noted that the estimated peak times did tend to be slightly longer for the uncued functions, despite the lack of significance. One aspect that also should be noted is that the task itself was rather simple, a contrast discrimination. The nature of the task would define this as a 'feature' search, in terms of Feature Integration Theory (Treisman & Gelade, 1980) and Guided Search (Wolfe, 1994, 2007; Wolfe et al., 1989; Wolfe & Gancarz, 1996), with the feature being contrast, and thus a parallel search under these theories. However, a priori, it was not necessarily apparent that a parallel model should best describe these results. It has been suggested that near-threshold discrimination tasks (such as the current study) are governed by serial and/or limited capacity attentional processes, most notably by Duncan and Humphreys (1989). Also, 'feature' tasks of the orientation of Gabor patches have been employed to suggest serial or limited capacity attentional processing, leading to delays at uncued locations (Carrasco et al., 2004, 2006; Carrasco & McElree, 2001).

In the studies by Carrasco et al. (Carrasco et al., 2004, 2006; Carrasco & McElree, 2001), speed-accuracy trade-off curves were generated by employing a 'deadline' procedure; observers had to respond within 300 ms or 350 ms of a tone occurring 40 ms–2000 ms after the stimulus. Signal locations were either cued with 100% validity, or not cued (a neutral condition), across set sizes of 1, 4, and 8. For the cued locations, the results indicated both higher asymptotes (indicating higher overall performance, or *d*'s) and faster rises to the asymptotes (suggesting speeded processing). While the current study did not manipulate response times, inferences and comparisons can be made to the deadline procedure of Carrasco et al. (Carrasco et al., 2004, 2006; Carrasco & McElree, 2001). Both findings of increased performance and speeded processing for the cued locations in these studies were represented in the classification number functions. First, increased performance was represented by the increased amplitudes of the cued functions. Second, speeded processing (as defined by Carrasco et al.) was represented by the greater initial rise of the cued functions, concurrent with the greater amplitudes. Note, however, that the same aspects were predicted well by the extended weighted likelihood model, a parallel-noisy model (Figure 11). The reason is that the weighted likelihood model considers both cued and uncued locations in its decision, compared to separate analyses at each location, as done by Carrasco et al. (Carrasco et al., 2004, 2006; Carrasco & McElree, 2001). Thus, the weighted likelihood model assumes the same sensitivity at each location, but with the differential (larger) weighting at the cued location. To repeat a point made earlier, the predicted differences between the cued and uncued classification number functions made by the extended weighted likelihood model are analogous to the differences in behavioral performance (expressed as valid hit rate − invalid hit rate) predicted by the weighted likelihood model (Table 1; Eckstein et al., 2002; Shimozaki et al., 2003). They are also analogous to the results found for spatial response classification (classification images) at

cued and uncued locations in Eckstein et al. (2002). In that study, they found that the cued classification images had greater amplitudes then the uncued classification images; however, these differences were predicted by the weighted likelihood model, and scaling the uncued classification images to match the amplitudes of the cued classification images resulted in no difference in shape, again as predicted by the weighted likelihood model.

A possible serial account for the results in the current study is a 'switching' hypothesis, in which the observer opts to switch his or her attention probabilistically, either to the cued or to the uncued location, from trial to trial and stays at the attended location (e. g., Shaw, 1982; Sperling & Melchner, 1978). A common model would be a switching rate equal to the cue validity (in this case, 80% to the cued location, and 20% to the uncued location). Such a model could not be directly assessed in the context of this study, but was assessed in Shimozaki et al. (2003), which estimated predictions of response rates as a function of signal contrast for the switching model (and the weighted likelihood model and another parallel-noisy model proposed by Kinchla et al., 1995). Shimozaki et al. (2003) differed from the current study, having static stimuli and different signals (Gaussian) and cues (precues appearing before the stimuli), but was similar in its task (cued contrast discrimination of Gaussian blobs), spatial configuration (2 locations) and cue validity (80%). The data from Shimozaki et al. (2003) study were an extremely poor fit to the predictions of the switching model (and were well fit to the weighted likelihood model). Given the extremely poor fits of the switching model in Shimozaki et al. (2003), and the relative similarity to the current study, it seems that switching would be an unlikely explanation for the current study.

VanRullen, Carlson, and Cavanagh (2007) proposed an alternative switching hypothesis in which attention switches and samples locations periodically about 7 items per second, or about once every 143 ms, even when attending a single location. Such a discrete or periodic sampling would seem to predict a drop in the classification number functions at or near 143 ms in the current study. This does not seem to be represented in the results, as most classification number functions appear to peak around this time (the one exception being SS). Also, the 4^{th}-degree polynomial fits did not significantly improve the fits given by the 3^{rd}-degree polynomials, as would be anticipated with a two-peak function predicted by the discrete sampling model within the stimulus duration for the current study. However, it should be noted that the periodic sampling in VanRullen et al. (2007) only occurred for more difficult discriminations, and parallel processing was found in easier discriminations. Also, their assessment was over a longer period of time (1 second), which may induce a more periodic sampling behavior than the shorter duration of the current study (272 ms).

For most observers and conditions, evidence of information use was found at the cued location in the first interval (22.7 ms). These results were consistent with a previous study by Shimozaki et al. (2007), using response classification in a cueing task with 100% valid cues, and finding evidence for first information use at the cued location at 37.5 to 75 ms. As mentioned earlier, this might be taken as an estimate of the latency of attentional processing (given that the cue was presented simultaneously with the stimulus duration). This estimate seems faster than previous estimates of the attentional latency, both from perceptual (e. g., Lyon, 1990; Mackeben & Nakayama, 1993; Nakayama & Mackeben, 1989), and from ERP studies (e.g., Clark & Hillyard, 1996; Harter, Miller, Price, LaLonde, & Keyes, 1989; Hillyard, Teder-Salejarvi, & Munte, 1998; Mangun, 1995; Martínez et al., 1999; Nobre, Sebestyen, & Miniussi, 2000), which give estimates of about 50–100 ms. One aspect of the response classification technique, however, is that the technique does not account for the temporal blurring of information expected from the visual system, due to the impulse response function. Essentially, this blurring extends the effective duration of information presented to an observer at a single point in time. This previous study (Shimozaki et al., 2007) modelled the effect of this blurring with a standard model of the impulse response function (Watson, 1986) and found that an adjustment of about 9–28 ms might be expected for the attentional latency from the response classification technique, which is more consistent with the other estimates.

Before fitting the classification number functions with the 3^{rd}-degree polynomials, fits were attempted with log-Gaussian and Poisson functions. These were attempted as representative functions with positive skew, which seemed to describe the basic characteristic of the classification number functions. Also, the log-Gaussian function was employed previously to fit equivalent classification number functions in saccadic decisions (Ludwig et al., 2005). The fits to the log-Gaussian and Poisson functions were relatively poor, particularly for the cued functions. For the log-Gaussian functions, the differences in the quality of fits, compared to Ludwig et al. (2005), could be due to several factors. The most obvious is the saccadic vs. attentional information use, but others include static conditions vs. temporal noise, slightly different assessments of fits (correlations instead of Hotelling T^2's), different signals (Gaussians vs. Gabors), the use of precues, and longer stimulus durations (500 ms and 1000 ms vs. 272 ms).

Conclusions

The temporal dynamics of information use were compared between the cued and uncued locations in a cueing task with the response classification (classification image) technique, with the primary goal of assessing whether visual attention operates serially or in parallel for

this task. The results from the response classification technique yield a single number for each location (cued and uncued) and interval in the stimulus duration (12 intervals in 272 ms); this number can be described as estimating the amount of information used in that interval at each location. Thus, for each observer there were two classification number functions, one at the cued location and one at the uncued location, estimating information use throughout the stimulus duration at the two locations. A serial attentional spotlight would suggest a delay in information use at the uncued location, relative to the cued location, whereas a parallel mechanism would not.

For the cueing task in this study, with two locations and an 80% valid cue presented simultaneously with the stimulus, a parallel account of attention seemed to provide a satisfactory account of the results from the classification number functions. After the uncued classification number functions were scaled to the same amplitude as the cued function, the two functions could not be distinguished. Also, estimates of the times for the peak amplitudes for the cued and uncued classification number functions (after smoothing with 3rd-degree polynomial functions) were not significantly different from each other. Thus, these classification number functions do not suggest a difference between the cued and uncued temporal dynamics in the form of a delay at the uncued location, and therefore did not indicate a serial attentional mechanism. There was a difference in the amplitudes and integrals of the classification number functions, with greater amplitudes and integrals for the cued locations. These differences in the classification number functions, however, could be predicted by a parallel-noisy model based upon the weighted likelihood model that assumed a linear integration of information across intervals.

Appendix A

Hotelling T^2 statistics

Comparisons between the overall classification number functions were performed with the Hotelling T^2 statistic (Harris, 1985). The Hotelling T^2 is the multivariate generalization of the univariate t statistic; analogous to the t statistic, the Hotelling T^2 has two forms, one-sample and two-sample. The one-sample Hotelling T^2 is appropriate for comparisons of a sample (multivariate) vector against a fixed or known population vector, such as differences of a sample vector from a hypothesized model or from zero. It is calculated as

$$T^2 = N[\mathbf{a}-\mathbf{a_0}]^t\mathbf{K}^{-1}[\mathbf{a}-\mathbf{a_0}], \tag{A1}$$

where T^2 is the Hotelling T^2 statistic, N = sample size, $\mathbf{a}$ = the sample vector (the classification number function), $\mathbf{a_0}$ = the population (model) vector, $[\mathbf{a} - \mathbf{a_0}]^t$ is the transpose of $[\mathbf{a} - \mathbf{a_0}]$, and $\mathbf{K}^{-1}$ is the inverse of the covariance matrix of the sample vector. For tests of significance, T^2 may be transformed into an F statistic by the following:

$$F = \frac{N-p}{p(N-1)}T^2, \tag{A2}$$

where p = length of the vector $[\mathbf{a} - \mathbf{a_0}]$, degrees of freedom ($df$) for the numerator ($df_{numerator}$) = p, and $df_{denominator} = N - p$.

The two-sample Hotelling T^2 is appropriate for comparisons of two sample vectors (classification number functions), and is calculated as

$$T^2 = \frac{N_1N_2}{N_1+N_2}[\mathbf{a_1}-\mathbf{a_2}]^t\mathbf{K}^{-1}[\mathbf{a_1}-\mathbf{a_2}]. \tag{A3}$$

where N_1 = the sample size for the first sample vector, N_2 = the sample size for the second sample vector, $\mathbf{a_1}$ = the first sample vector, and $\mathbf{a_2}$ = the second sample vector. The covariance matrix $\mathbf{K}$ is computed as the pooled variances/covariances across $\mathbf{a_1}$ and $\mathbf{a_2}$. The corresponding F statistic is computed as

$$F = \frac{N_1+N_2+p-1}{p(N_1+N_2-2)}T^2 \tag{A4}$$

with $df_{numerator} = p$, and $df_{denominator} = N_1 + N_2 - p - 1$.

For the one-sample Hotelling T^2 statistic with a diagonal covariance matrix $\mathbf{K}$ (i.e., all zero correlations), the T^2 statistic may be described as

$$T^2 = \sum_{i=1}^{H}\frac{(a_i-a_{0,i})^2}{(\frac{\sigma_{a_i}}{N})^2} = \sum_{i=1}^{H}\frac{(a_i-a_{0,i})^2}{(\sigma_{\bar{a}_i})^2} \tag{A5}$$

where H = the number of intervals = 12. This is distributed as a χ^2 statistic for differences between the sample classification number function ($\mathbf{a}$) and a hypothesized model ($\mathbf{a_0}$). It was found that the correlations across intervals for the classification number functions were nearly zero (mean across observers = −0.002, with a range from −0.053 to 0.034), and not significantly different from zero for any observer. Across observers, the single-sample t values for differences from zero ranged from 1.037 to 1.604, giving p-values ranging from 0.3302 to 0.1092. Thus, for comparisons of hypothesized models (with q = number of free parameters) against the

sample classification number functions, the one-sample Hotelling T^2 statistics were evaluated as χ^2 statistics for the model, and $df = p - q$.

Appendix B

Behavioral results

See Table B1.

Appendix C

Classification number functions

See Table C1.
See Table C2.

Appendix D

Fits of the classification number functions

Table D1 gives the fits of the classification number functions to the 3rd-degree polynomials of the form

$$f(t) = c_0 + c_1 t + c_2 t^2 + c_3 t^3, \quad \text{(D1)}$$

These fits are presented in Figure 9. All polynomial fits were not significantly different from the raw classification number functions, except for the uncued function for SS, which had an uncharacteristic 'dip' compared to other functions at 158.7 ms.

Aside from polynomials, two functions with positive skew were attempted to fit and smooth the classification number functions, log-Gaussian and Poisson. A log-Gaussian function was used previously for analogous functions in saccadic decisions by Ludwig et al. (2005), defined as a function of time (t):

$$f(t) = c_0 + c_1 e^{\left(-\frac{1}{2}\left(\frac{\ln(t/c_2)}{c_3}\right)^2\right)}. \quad \text{(D2)}$$

For this function, c_0 equals the y-offset, c_1 equals the peak amplitude, c_2 determines the peak time (the 'location'), and c_3 equals the spread or 'scale.' The second function was a Poisson, defined as a function of interval (i):

$$f(i) = c_0 + c_1 \frac{c_2^i e^{-c_2}}{i!}. \quad \text{(D3)}$$

For this function, c_0 equals the y-offset, c_1 determines the peak amplitude, and c_2 is the mean and the variance.

Table D2 gives the data fits to the log-Gaussian (Table D2a) and Poisson functions (Table D2b), assessed with one-sample Hotelling T^2 statistics evaluated as χ^2's

Table B1a

Observer	Proportion correct	Valid hit rate	Invalid hit rate	False alarm rate
AW	0.7921	0.8048	0.6185	0.2906
FB	0.7508	0.7537	0.6531	0.2307
LO	0.7372	0.8768	0.7404	0.2635
SS	0.7543	0.8037	0.6323	0.2588

Table B1b

Observer	Cueing (valid hit − invalid hit)	$\chi^2(1)$	p-value	Sig.
AW	0.1863	414.2	0.0000	*
FB	0.1006	118.5	0.0000	*
LO	0.1364	293.7	0.0000	*
SS	0.1714	354.3	0.0000	*

Table B1. Behavioral performance for the observers, summarized in Figure 6. B1a. False alarm, valid hit rates, and invalid hit rates. B1b. Cueing effects, assessed as valid hit rate − invalid hit rate. The difference of cueing effects were assessed as a difference of the valid hit rate and the invalid hit rate with χ^2 and degrees of freedom = 1. *Note*: * = $p < .05$.

AW (n = 9779)

Time (ms)	Cued			Diff. from zero		Uncued			Diff. from zero	
	Class. Number	*SE*	*t*	*p*	Sig.	Class. Number	*SE*	*t*	*p*	Sig.
22.7	0.916	0.351	2.606	0.0092	*	1.207	0.353	3.421	0.0006	*
45.3	3.193	0.343	9.314	0.0000	*	0.957	0.348	2.749	0.0060	*
68.0	4.428	0.343	12.916	0.0000	*	0.686	0.353	1.940	0.0523	
90.7	3.480	0.347	10.035	0.0000	*	0.986	0.346	2.852	0.0043	*
113.3	4.011	0.346	11.608	0.0000	*	1.277	0.350	3.649	0.0003	*
136.0	3.911	0.350	11.166	0.0000	*	1.540	0.353	4.362	0.0000	*
158.7	2.955	0.350	8.442	0.0000	*	0.958	0.344	2.788	0.0053	*
181.3	2.540	0.347	7.326	0.0000	*	1.309	0.347	3.771	0.0002	*
204.0	2.384	0.356	6.705	0.0000	*	0.850	0.339	2.507	0.0122	
226.7	1.108	0.344	3.217	0.0013	*	0.746	0.348	2.146	0.0318	
249.3	1.138	0.347	3.277	0.0011	*	0.706	0.350	2.018	0.0436	
272.0	1.261	0.350	3.603	0.0003	*	0.283	0.346	0.817	0.4140	

Time (ms)	Cued vs. Uncued			Scaled Uncued scale factor = 0.33	
	t	*p*	Sig.	Class. Number	*SE*
22.7	−0.585	0.5584		3.658	1.069
45.3	4.576	0.0000	*	2.900	1.055
68.0	7.599	0.0000	*	2.079	1.071
90.7	5.093	0.0000	*	2.988	1.048
113.3	5.561	0.0000	*	3.868	1.060
136.0	4.768	0.0000	*	4.666	1.070
158.7	4.072	0.0000	*	2.903	1.041
181.3	2.508	0.0121		3.968	1.052
204.0	3.123	0.0018	*	2.576	1.028
226.7	0.739	0.4597		2.261	1.053
249.3	0.876	0.3809		2.140	1.060
272.0	1.987	0.0469		0.857	1.049

FB (n = 9779)

Time (ms)	Cued			Diff. from zero		Uncued			Diff. from zero	
	Class. Number	*SE*	*t*	*p*	Sig.	Class. Number	*SE*	*t*	*p*	Sig.
22.7	0.210	0.378	0.556	0.5783		−0.173	0.381	0.455	0.6490	
45.3	2.077	0.371	5.595	0.0000	*	0.261	0.375	0.696	0.4862	
68.0	2.322	0.372	6.240	0.0000	*	1.538	0.381	4.031	0.0001	*
90.7	3.098	0.374	8.273	0.0000	*	1.966	0.372	5.291	0.0000	*
113.3	3.345	0.373	8.970	0.0000	*	1.513	0.378	4.005	0.0001	*
136.0	3.813	0.377	10.102	0.0000	*	2.057	0.379	5.422	0.0000	*
158.7	2.523	0.378	6.680	0.0000	*	1.338	0.370	3.613	0.0003	*
181.3	2.203	0.373	5.900	0.0000	*	2.140	0.374	5.717	0.0000	*
204.0	1.897	0.383	4.951	0.0000	*	1.152	0.365	3.157	0.0016	*
226.7	1.945	0.371	5.242	0.0000	*	1.327	0.375	3.541	0.0004	*
249.3	2.238	0.375	5.975	0.0000	*	1.085	0.378	2.872	0.0041	*
272.0	1.742	0.376	4.634	0.0000	*	1.016	0.372	2.731	0.0063	*

Time (ms)	Cued vs. Uncued			Scaled Uncued scale factor = 0.57	
	t	*p*	Sig.	Class. Number	*SE*
22.7	0.715	0.4748		−0.304	0.669
45.3	3.443	0.0006	*	0.458	0.657
68.0	1.472	0.1410		2.697	0.669
90.7	2.144	0.0320		3.450	0.652
113.3	3.452	0.0006	*	2.654	0.663
136.0	3.281	0.0010	*	3.609	0.666
158.7	2.242	0.0249		2.347	0.649
181.3	0.120	0.9047		3.754	0.657
204.0	1.407	0.1594		2.022	0.640
226.7	1.173	0.2406		2.327	0.657
249.3	2.167	0.0302		1.904	0.663
272.0	1.372	0.1701		1.783	0.653

LO (*n* = 9804)

Time (ms)	Cued		Diff. from zero			Uncued		Diff. from zero		
	Class. Number	*SE*	*t*	*p*	Sig.	Class. Number	*SE*	*t*	*p*	Sig.
22.7	0.837	0.362	2.313	0.0207	*	0.789	0.363	2.173	0.0298	
45.3	3.648	0.353	10.325	0.0000	*	1.691	0.358	4.730	0.0000	*
68.0	5.373	0.352	15.263	0.0000	*	1.313	0.364	3.601	0.0003	*
90.7	4.912	0.356	13.814	0.0000	*	2.205	0.355	6.217	0.0000	*
113.3	5.130	0.354	14.475	0.0000	*	1.842	0.360	5.120	0.0000	*
136.0	5.307	0.359	14.798	0.0000	*	2.548	0.363	7.021	0.0000	*
158.7	4.196	0.359	11.699	0.0000	*	1.802	0.354	5.086	0.0000	*
181.3	4.240	0.355	11.957	0.0000	*	2.202	0.357	6.168	0.0000	*
204.0	3.276	0.366	8.961	0.0000	*	1.052	0.349	3.010	0.0026	*
226.7	1.972	0.355	5.552	0.0000	*	0.870	0.358	2.432	0.0150	*
249.3	1.880	0.358	5.258	0.0000	*	1.044	0.361	2.893	0.0038	*
272.0	1.087	0.360	3.023	0.0025	*	0.691	0.356	1.941	0.0523	

Time (ms)	Cued vs. Uncued			Scaled Uncued scale factor = 0.42	
	t	*p*	Sig.	Class. Number	*SE*
22.7	0.093	0.9259		1.879	0.865
45.3	3.893	0.0001	*	4.027	0.851
68.0	8.013	0.0000	*	3.125	0.868
90.7	5.391	0.0000	*	5.249	0.844
113.3	6.511	0.0000	*	4.386	0.857
136.0	5.406	0.0000	*	6.068	0.864
158.7	4.750	0.0000	*	4.289	0.843
181.3	4.051	0.0001	*	5.242	0.850
204.0	4.399	0.0000	*	2.504	0.832
226.7	2.185	0.0289		2.072	0.852
249.3	1.647	0.0996		2.485	0.859
272.0	0.783	0.4336		1.644	0.847

SS (n = 9832)

Time (ms)	Cued			Diff. from zero		Uncued			Diff. from zero	
	Class. Number	*SE*	*t*	*p*	Sig.	Class. Number	*SE*	*t*	*p*	Sig.
22.7	1.273	0.357	3.568	0.0004	*	1.305	0.365	3.578	0.0003	*
45.3	3.457	0.357	9.674	0.0000	*	1.299	0.355	3.663	0.0002	*
68.0	4.609	0.353	13.042	0.0000	*	1.894	0.364	5.196	0.0000	*
90.7	4.855	0.354	13.702	0.0000	*	2.305	0.360	6.411	0.0000	*
113.3	4.640	0.360	12.905	0.0000	*	2.690	0.365	7.365	0.0000	*
136.0	5.700	0.358	15.913	0.0000	*	2.930	0.367	7.979	0.0000	*
158.7	5.055	0.355	14.232	0.0000	*	1.073	0.362	2.961	0.0031	*
181.3	3.936	0.354	11.114	0.0000	*	1.959	0.358	5.478	0.0000	*
204.0	3.645	0.361	10.103	0.0000	*	1.702	0.353	4.816	0.0000	*
226.7	3.283	0.360	9.124	0.0000	*	2.267	0.358	6.329	0.0000	*
249.3	3.266	0.360	9.061	0.0000	*	1.289	0.357	3.615	0.0003	*
272.0	1.744	0.360	4.842	0.0000	*	0.307	0.357	0.860	0.3895	

Time (ms)	Cued vs. Uncued			Scaled Uncued scale factor = 0.46	
	t	*p*	Sig.	Class. Number	*SE*
22.7	−0.063	0.9499		2.836	0.793
45.3	4.286	0.0000	*	2.824	0.771
68.0	5.349	0.0000	*	4.117	0.792
90.7	5.049	0.0000	*	5.012	0.782
113.3	3.805	0.0001	*	5.848	0.794
136.0	5.399	0.0000	*	6.371	0.798
158.7	7.850	0.0000	*	2.332	0.788
181.3	3.929	0.0001	*	4.258	0.777
204.0	3.845	0.0001	*	3.701	0.769
226.7	2.000	0.0455		4.929	0.779
249.3	3.899	0.0001	*	2.802	0.775
272.0	2.834	0.0046	*	0.668	0.776

Table C1. The classification number functions for each observer. The scaled uncued functions were found by matching the amplitudes of the uncued functions to provide the best fit to the cued functions, as assessed by two-sample Hotelling T^2 statistics. Each interval was assessed for differences from zero by single-sample *t*-tests, adjusted for 12 multiple comparisons by the Simes-Hochberg method (Hochberg, 1988; Simes, 1986). Each interval was assessed for differences between the cued and uncued classification numbers by independent-sample *t*-tests, adjusted for 12 multiple comparisons by the Simes-Hochberg method (Hochberg, 1988; Simes, 1986).

Table C2a

Observer		Hotelling T^2	df_2	$F(12,df_2)$	p-value	Sig.
AW	cued	815.36	9767	67.870	0.0000	*
	uncued	63.46	9767	5.283	0.0000	*
FB	cued	514.48	9767	42.825	0.0000	*
	uncued	107.52	9767	8.950	0.0000	*
LO	cued	1379.74	9792	114.849	0.0000	*
	uncued	153.05	9792	12.740	0.0000	*
SS	cued	1483.28	9820	123.468	0.0000	*
	uncued	203.08	9820	16.904	0.0000	*

Table C2b

Observer	Hotelling T^2	df_2	$F(12,df_2)$	p-value	Sig.
AW	146.04	19545	12.163	0.0000	*
FB	43.31	19545	3.607	0.0000	*
LO	184.23	19595	15.344	0.0000	*
SS	177.81	19651	14.809	0.0000	*

Table C2. Analyses of the classification number functions. C2a. Tests for differences from zero, as assessed by one-sample Hotelling T^2 statistics. C2b. Tests for differences between the cued and uncued functions for each observer, as assessed by two-sample Hotelling T^2 statistics. *Note*: * = $p < .05$.

Observer		Hotelling T^2	df	p-value	Sig.	$c0$	$c1$	$c2$	$c3$
AW	cued	12.78	8	0.1196		−1.19	125.63	−884.1	1674.4
	uncued	3.82	8	0.8730		1.17	−6.83	85.6	−268.7
FB	cued	8.27	8	0.4076		−1.83	108.45	−707.8	1327.5
	uncued	7.32	8	0.5025		−1.56	63.99	−368.3	618.0
LO	cued	13.19	8	0.1055		−1.79	153.95	−983.0	1684.5
	uncued	9.22	8	0.3241		−0.04	43.16	−255.3	389.5
SS	cued	13.60	8	0.0928		−0.77	115.11	−664.7	1032.3
	uncued	21.12	8	0.0068	*	0.65	25.85	−103.0	27.0

Table D1. Summary of the 3rd-degree polynomial fits to the classification number functions. Fits were assessed as one-sample Hotelling T^2 statistics, evaluated as χ^2 with degrees of freedom = 12 − p = 12 − 4 = 8, where p = number of free parameters. Coefficients were fit with respect to t = time in seconds. *Note*: * = $p < .05$.

Table D2a

Observer		Hotelling T^2	*df*	*p*-value	Sig.	*c*0	*c*1	*c*2	*c*3
AW	cued	28.16	8	0.0004	*	0.44	5.25	61	0.90
	uncued	13.40	8	0.0989		0.99	1.34	92	−0.43
FB	cued	11.09	8	0.1965		0.23	2.96	76	1.03
	uncued	6.12	8	0.6335		−0.23	2.14	92	0.93
LO	cued	18.28	8	0.0192	*	0.62	3.75	53	0.89
	uncued	5.55	8	0.6970		0.78	0.65	106	−0.28
SS	cued	23.72	8	0.0026	*	1.12	4.18	71	0.93
	uncued	23.24	8	0.0031	*	1.14	1.50	83	−0.49

Table D2b

Observer		Hotelling T^2	*df*	*p*-value	Sig.	*c*0	*c*1	*c*2
AW	cued	37.19	9	0.0000	*	1.39	25.31	5.45
	uncued	9.21	9	0.4181		0.75	9.27	5.88
FB	cued	20.85	9	0.0133	*	1.20	13.18	5.96
	uncued	15.27	9	0.0838		0.44	10.11	6.81
LO	cued	24.20	9	0.0040	*	1.13	17.78	4.99
	uncued	6.21	9	0.7187		0.64	3.92	6.13
SS	cued	29.08	9	0.0006	*	2.03	21.30	6.03
	uncued	23.68	9	0.0048	*	1.01	9.02	5.74

Table D2. Summary of the log-Gaussian and Poisson fits to the classification number functions. Fits were assessed as one-sample Hotelling T^2 statistics, evaluated as χ^2 with degrees of freedom = 12 − *p,* where *p* = number of free parameters. D2a. The log-Gaussian fits as a function of *t* = time in milliseconds, with degrees of freedom = 12 − 4 = 8. D2b. The Poisson fits as a function of *i* = interval (1 to 12). *Note*: * = $p < .05$.

and with degrees of freedom = 12 − number of free parameters. Thus, the log-Gaussian fits had 12 − 4 = 8 degrees of freedom, and the Poisson fits had 12 − 3 = 9 degrees of freedom. Table D2 also summarizes the free parameters for the functions, in terms of milliseconds for the log-Gaussian fits, and in terms of interval (1 to 12) for the Poisson fits. Across both functions the fits for the cued functions were generally poor, with significant differences found for all but one fit (FB, log-Gaussian). The fits for the uncued functions tended to be better, with no significant differences found across observers, except for SS.

Appendix E

Fits to the extended weighted likelihood model

See Table E1.
See Table E2.

Observer	$\chi^2(3)$	*p*-value	Sig.
AW	1.103	0.7764	
FB	0.454	0.9288	
LO	0.715	0.8696	
SS	0.932	0.8177	

Table E1. Fits of the predicted behavioral responses from the extended weighted likelihood model to the original response rates of the observers. Fits were performed on the response rates, i.e., valid hit and miss rates, invalid hit and miss rates, false alarm rates, and correct rejection rates. *Note*: * = $p < .05$.

Observer	Hotelling T^2	df_2	$F(12,df_2)$	*p*-value	Sig.
AW	cued	0.463	19595	0.039	0.9999
FB	cued	0.169	19545	0.014	0.9999
LO	cued	0.199	19545	0.017	0.9999
SS	cued	2.684	19651	0.224	0.9974

Table E2. Fits of the predicted classification number functions from the extended weighted likelihood model to the 3rd-degree polynomial functions for the cued locations (Table 6). The fits were evaluated with two-sample Hotelling T^2 statistics using the covariance matrices from the original classification number functions. *Note*: * = $p < .05$.

Acknowledgments

The author would like to thank Miguel Eckstein, Craig Abbey, and Barry Giesbrecht for their advice, and special thanks to Jocelyn Sy for programming assistance. The author would like to thank Lorraine O'hara, Frances Billington, and Alice Woodward for their patient participation in the study. This study was partially funded by the Seed Corn Fund, School of Psychology, University of Leicester, UK.

Commercial relationships: none.
Corresponding author: Steven S. Shimozaki.
Email: ss373@le.ac.uk.
Address: School of Psychology, University of Leicester, Lancaster Road, Leicester, LE1 9HN, United Kingdom.

References

Ahumada, A. J., Jr. (2002). Classification image weights and internal noise level estimation. *Journal of Vision, 2*(1):8, 121–131, http://www.journalofvision.org/content/2/1/8, doi:10.1167/2.1.8. [PubMed] [Article]

Ahumada, A. J., & Lovell, J. (1971). Stimulus features in signal detection. *Journal of the Acoustical Society of America, 49,* 1751–1756.

Awh, E., & Pashler, H. (2000). Evidence for split attentional foci. *Journal of Experimental Psychology: Human Perception & Performance, 26,* 834–846. [PubMed]

Bichot, N. P., Cave, K. R., & Pashler, H. (1999). Visual selection mediated by location: Feature-based selection of noncontiguous locations. *Perception & Psychophysics, 61,* 403–423. [PubMed]

Brainard, D. H. (1997). The psychophysics toolbox. *Spatial Vision, 10,* 433–436. [PubMed]

Carrasco, M., Giordano, A. M., & McElree, B. (2004). Temporal performance fields: Visual and attentional factors. *Vision Research, 44,* 1351–1365. [PubMed]

Carrasco, M., Giordano, A. M., & McElree, B. (2006). Attention speeds processing across eccentricity: Feature and conjunction searches. *Vision Research, 46,* 2028–2040. [PubMed]

Carrasco, M., & McElree, B. (2001). Covert attention accelerates the rate of visual information processing. *Proceedings of the National Academy of Sciences of the United States of America, 98,* 5363–5367. [PubMed] [Article]

Carrasco, M., Williams, P. E., & Yeshurun, Y. (2002). Covert attention increases spatial resolution with or without masks: Support for signal enhancement. *Journal of Vision, 2*(6):4, 467–479, http://www.journalofvision.org/content/2/6/4, doi:10.1167/2.6.4. [PubMed] [Article]

Caspi, A., Beutter, B. R., & Eckstein, M. P. (2004). The time course of visual information accrual guiding eye movement decisions. *Proceedings of the National Academy of Sciences of the United States of America, 101,* 13086–13090. [PubMed] [Article]

Clark, V. P., & Hillyard, S. A. (1996). Spatial selective attention affects early exastriate but not striate components of visual evoked potential. *Journal of Cognitive Neuroscience, 8,* 387–402.

Droll, J. A., Abbey, C. K., & Eckstein, M. P. (2009). Learning cue validity through performance feedback. *Journal of Vision, 9*(2):18, 1–22, http://www.journalofvision.org/content/9/2/18, doi:10.1167/9.2.18. [PubMed] [Article]

Duncan, J., & Humphreys, G. W. (1989). Visual search and stimulus similarity. *Psychological Review, 96,* 433–458. [PubMed]

Eckstein, M. P., & Ahumada, A. J., Jr. (2002). Classification images: A tool to analyze visual strategies. *Journal of Vision, 2*(1):i, i, http://www.journalofvision.org/content/2/1/i, doi:10.1167/2.1.i. [PubMed] [Article]

Eckstein, M. P., Peterson, M. F., Pham, B. T., & Droll, J. A. (2009). Statistical decision theory to relate neurons to behavior in the study of covert visual attention. *Vision Research, 49,* 1097–1128. [PubMed]

Eckstein, M. P., Shimozaki, S. S., & Abbey, C. K. (2002). The footprints of visual attention in the Posner cueing paradigm revealed by classification images. *Journal of Vision, 2*(1):3, 25–45, http://www.journalofvision.org/content/2/1/3, doi:10.1167/2.1.3. [PubMed] [Article]

Eckstein, M. P., Thomas, J. P., Palmer, J., & Shimozaki, S. S. (2000). A signal detection model predicts the effects of set size on visual search accuracy for feature, conjunction, triple conjunction, and disjunction displays. *Perception & Psychophysics, 62,* 425–451. [PubMed]

Efron, B., & Tibshirani, R. (1993). *An introduction to the bootstrap*. New York: Chapman and Hall.

Eriksen, C. W., & St. James, J. D. (1986). Visual attention within and around the field of focal attention: A zoom lens model. *Perception & Psychophysics, 40,* 225–240. [PubMed]

Eriksen, C. W., & Yeh, Y. Y. (1985). Allocation of attention in the visual field. *Journal of Experimental Psychology: Human Perception & Performance, 11,* 583–597. [PubMed]

Folk, C. L., Remington, R. W., & Johnston, J. C. (1992). Involuntary covert orienting is contingent on attentional control settings. *Journal of Experimental Psychology: Human Perception & Performance, 18,* 1030–1044. [PubMed]

Ghose, G. M. (2006). Strategies optimize the detection of motion transients. *Journal of Vision, 6*(4):10, 429–440,

http://www.journalofvision.org/content/6/4/10, doi:10.1167/6.4.10. [PubMed] [Article]

Golla, H., Ignashchenkova, A., Haarmeier, T., & Thier, P. (2004). Improvement of visual acuity by spatial cueing: A comparative study in human and non-human primates. *Vision Research, 44,* 1589–1600. [PubMed]

Harris, R. J. (1985). *A primer of multivariate statistics* (pp. 99–118). Orlando, FL: Academic Press.

Harter, M. R., Miller, S. L., Price, N. J., LaLonde, M. E., & Keyes, A. L. (1989). Neural processes involved in directing attention. *Journal of Cognitive Neuroscience, 1,* 223–237.

Hillyard, S. A., Teder-Salejarvi, W. A., & Munte, T. F. (1998). Temporal dynamics of early perceptual processing. *Current Opinion in Neurobiology, 8,* 202–210. [PubMed]

Hochberg, Y. (1988). A sharper Bonferroni procedure for multiple tests of significance. *Biometrika, 75,* 800–802.

Jones, J. P., & Palmer, L. A. (1987). The two-dimensional spatial structure of simple receptive fields in cat striate cortex. *Journal of Neurophysiology, 58,* 1187–1211. [PubMed]

Jonides, J. (1981). Voluntary vs. automatic control 'over the mind's eye's movement. In J. B. Long & A. D. Baddeley (Eds.), *Attention and performance IX* (pp. 187–203). Hillsdale, NJ: Erlbaum.

Kinchla, R. A. (1974). Detecting target elements in multielement arrays: A confusability model. *Perception & Psychophysics, 15,* 149–158.

Kinchla, R. A., Chen, Z., & Evert, D. (1995). Precue effects in visual search: Data or resource limited? *Perception & Psychophysics, 57,* 441–450. [PubMed]

Kramer, A. F., & Hahn, S. (1995). Splitting the beam: Distribution of attention over noncontiguous regions of the visual field. *Psychological Science, 6,* 381–386.

Ludwig, C. J. H., Gilchrist, I. D., McSorley, E., & Baddeley, R. J. (2005). The temporal impulse response underlying saccadic decisions. *Journal of Neuroscience, 25,* 9907–9912. [PubMed] [Article]

Lyon, D. R. (1990). Large and rapid improvement in form discrimination accuracy following a location precue. *Acta Psychologica, 73,* 69–82. [PubMed]

Mackeben, M., & Nakayama, K. (1993). Express attentional shifts. *Vision Research, 33,* 85–90. [PubMed]

Mangun, G. R. (1995). Neural mechanisms of visual selective attention. *Psychophysiology, 32,* 4–18. [PubMed]

Martínez, A., Anllo-Vento, L., Sereno, M. I., Frank, L. R., Buxton, R. B., Dubowitz, D. J., et al. (1999). Involvement of striate and extrastriate visual cortical areas in spatial attention. *Nature Neuroscience, 4,* 364–369. [PubMed]

McMains, S. A., & Somers, D. C. (2004). Multiple spotlights of attentional selection in human visual cortex. *Neuron, 42,* 677–686. [PubMed]

McMains, S. A., & Somers, D. C. (2005). Processing efficiency of divided spatial attention mechanisms in human visual cortex. *Journal of Neuroscience, 25,* 9444–9448. [PubMed]

Montagna, B., Pestilli, F., & Carrasco, M. (2009). Attention trades off spatial acuity. *Vision Research, 49,* 735–745. [PubMed]

Müller, H. J., & Rabbitt, P. M. A. (1989). Reflexive and voluntary orienting of visual attention: Time course of activation and resistance to interruption. *Journal of Experimental Psychology: Human Perception and Performance, 15,* 315–330. [PubMed]

Müller, M. M., Malinowski, P., Gruber, T., & Hillyard, S. A. (2003). Sustained division of the attentional spotlight. *Nature, 424,* 309–312. [PubMed]

Murray, R. F., Bennett, P. J., & Sekuler, A. B. (2002). Optimal methods for calculating classification images: Weighted sums. *Journal of Vision, 2*(1):6, 79–104, http://www.journalofvision.org/content/2/1/6, doi:10.1167/2.1.6. [PubMed] [Article]

Nakayama, K., & Mackeben, M. (1989). Sustained and transient components of focal visual attention. *Vision Research, 29,* 1631–1647. [PubMed]

Neri, P., & Heeger, D. J. (2002). Spatiotemporal mechanisms for detecting and identifying image features in human vision. *Nature Neuroscience, 5,* 812–816. [PubMed]

Nobre, A. C., Sebestyen, G. N., & Miniussi, C. (2000). The dynamics of shifting visuospatial attention revealed by event-related potentials. *Neuropsychologia, 38,* 964–974. [PubMed]

Palmer, J. (1995). Attention in visual search: Distinguishing four causes of set-size effects. *Current Directions in Psychological Science, 4,* 118–123.

Palmer, J., Ames, C. T., & Lindsey, D. T. (1993). Measuring the effect of attention on simple visual search. *Journal of Experimental Psychology: Human Perception and Performance, 19,* 108–130. [PubMed]

Palmer, J., Verghese, P., & Pavel, M. (2000). The psychophysics of visual search. *Vision Research, 40,* 1227–1268. [PubMed]

Pelli, D. G. (1997). The VideoToolbox software for visual psychophysics: Transforming numbers into movies. *Spatial Vision, 10,* 437–442. [PubMed]

Posner, M. I. (1980). Orienting of attention. *Quarterly Journal of Experimental Psychology, 32,* 3–25.

Ringach, D. L., Sapiro, G., & Shapley, R. (1997). A subspace reverse-correlation technique for the study of visual neurons. *Vision Research, 37,* 2455–2464. [PubMed]

Shaw, M. L. (1980). Identifying attentional decision-making components in information processing. In R. S. Nickerson (Ed.), *Attention and performance, VIII* (pp. 277–296). Hillsdale, NJ: Lawrence Erlbaum Associates.

Shaw, M. L. (1982). Attending to multiple sources of information: 1. The integration of information in decision-making. *Cognitive Psychology, 14,* 353–409.

Shimozaki, S. S., Chen, K. Y., Abbey, C. K., & Eckstein, M. P. (2007). The temporal dynamics of selective attention of the visual periphery as measured by classification images. *Journal of Vision, 7*(12):10, 1–20, http://www.journalofvision.org/content/7/12/10, doi:10.1167/7.12.10. [PubMed] [Article]

Shimozaki, S. S., Eckstein, M. P., & Abbey, C. K. (2003). Comparison of two weighted integration models for the cueing paradigm: Linear and likelihood. *Journal of Vision, 3*(3):3, 209–229, http://www.journalofvision.org/content/3/3/3, doi:10.1167/3.3.3. [PubMed] [Article]

Simes, R. J. (1986). An improved Bonferroni procedure for multiple tests of significance. *Biometrika, 73,* 751–754.

Sperling, G., & Melchner, M. J. (1978). The attention operating characteristic: Examples from visual search. *Science, 202,* 315–318. [PubMed]

Spitzer, H., Desimone, R., & Moran, J. (1988). Increased attention enhances both behavioral and neuronal performance. *Science, 240,* 338–340. [PubMed]

Theeuwes, J. (1991). Exogenous and endogenous control of visual attention: The effect of visual onsets and offsets. *Perception & Psychophysics, 49,* 83–90. [PubMed]

Treisman, A., & Gelade, G. (1980). A feature-integration theory of attention. *Cognitive Psychology, 12,* 97–136. [PubMed]

VanRullen, R., Carlson, T., & Cavanagh, P. (2007). The blinking spotlight of attention. *Proceedings of the National Academy of Sciences of the United States of America, 104,* 19204–19209. [PubMed] [Article]

Verghese, P. (2001). Visual search and attention: A signal detection theory approach. *Neuron, 31,* 523–535. [PubMed]

Watson, A. B. (1986). Temporal sensitivity. In K. Boff, L. Kaufman, & J. P. Thomas (Eds.), *Handbook of perception and human performance* (Chapter 6). New York: Wiley.

Wolfe, J. M. (1994). Guided Search 2.0: A revised model of visual search. *Psychonomic Bulletin & Review, 1,* 202–238.

Wolfe, J. M. (2007). Guided search 4.0: Current progress with a model of visual search. In W. Gray (Ed.), *Integrated models of cognitive systems* (pp. 99–119). New York: Oxford University Press.

Wolfe, J. M., Cave, K. R., & Franzel, S. L. (1989). Guided Search: An alternative to the feature integration model for visual search. *Journal of Experimental Psychology: Human Perception and Performance, 15,* 419–433. [PubMed]

Wolfe, J. M., & Gancarz, G. (1996). Guided Search 3.0. In V. Lakshminarayanan (Ed.), *Basic and clinical applications of vision science* (pp. 189–192). Dordrecht, Netherlands: Kluwer Academic.

Wright, R. D., & Ward, L. M. (2008). Studying attention shifts with location cueing. In R. D. Wright & L. M. Ward (Eds.), *Orienting of attention* (pp. 15–36). Oxford: Oxford University Press.

Yeshurun, Y., & Carrasco, M. (1998). Attention improves or impairs visual performance by enhancing spatial resolution. *Nature, 396,* 72–76. [PubMed]

Yeshurun, Y., & Carrasco, M. (1999). Spatial attention improves performance in spatial resolution tasks. *Vision Research, 39,* 293–306. [PubMed]